

# Are We Measuring Strategy or Phrasing? The Gap Between Surface- and Approach-Level Diversity in LLM Math Reasoning

Sangmook Lee<sup>1</sup>, Minbeom Kim<sup>1</sup>, Jeonghye Kim<sup>2</sup>,  
Dohyung Kim<sup>1</sup>, Sojeong Rhee<sup>2</sup>, Kyomin Jung<sup>1</sup>

<sup>1</sup>Seoul National University, <sup>2</sup>KAIST

## Abstract

Diversity in LLM mathematical reasoning is critical for exploration, but common diversity metrics mostly capture *surface-level variation* rather than differences in how a problem is solved. We address this gap by introducing **approach-level diversity**: variation in strategies across correct solutions to the same problem. Using a human-calibrated LLM judge framework, we show that prior diversity measures are unreliable proxies for approach-level diversity, and this mismatch carries over to diversity-aware RLVR, where target metrics are preserved while approach-level diversity declines. Investigating when approach-level diversity helps and whether it can be directly induced, we find that approach-diverse candidate sets improve test-time scaling. However, optimizing an LLM judge diversity reward during training causes the policy to exploit judge-specific preferences rather than broaden its approaches, leaving direct optimization of approach-level diversity as an open problem. Together, our work introduces the notion of approach-level diversity and uncovers a systematic divergence between surface- and approach-level signals, marking a step toward LLMs that reason in genuinely diverse, human-like ways.

## 1 Introduction

Diversity in large language models (LLM) generations has become practically important across tasks where useful outputs span a range of plausible alternatives, such as creative writing (Gómez-Rodríguez and Williams, 2023) and synthetic data construction (Shumailov et al., 2024). In complex reasoning tasks, this importance is amplified by test-time scaling methods such as verifier-based selection (Lightman et al., 2023) and multi-agent collaboration (Wu et al., 2024a), where downstream performance depends on the range of candidate solutions sampled from the model.

However, recent studies report that reinforcement learning with verifiable rewards (RLVR), a

dominant paradigm for post-training language models, reduces the diversity of a trained policy (Kirk et al., 2024; He et al., 2025; Yue et al., 2025; Wu and Choi, 2025), prompting diversity-aware RLVR methods that attempt to preserve diversity during training. Yet we find that these methods typically operationalize diversity by *surface-level diversity*—differences in the observable form of outputs—through measures such as lexical overlap (Lanchantin et al., 2025), embedding distance (Chen et al., 2026), or symbolic representations like the ratio of unique equations (Hu et al., 2026). Such measures reveal whether solutions differ in wording or representation, but leave open a more fundamental question: *are models producing surface-level variants of the same strategy, or exploring genuinely different ways to solve the problem?*

To address this gap, we introduce **approach-level diversity** as a distinct axis of LLM reasoning behavior: variation in the underlying solution strategies used to arrive at the correct answer, beyond differences in wording, notation, or exposition. Prior work measures diversity at two common levels: lexical, typically via N-gram distance, and semantic, typically via cosine similarity over embeddings. We first evaluate whether these standard metrics align with human judgments of approach-level diversity. We find that these metrics are susceptible to paraphrastic variation in math reasoning, where changes in wording, layout, or symbolic expression can inflate the apparent diversity among solutions with the same reasoning approach.

Building on these observations, we design a scalable evaluation framework for approach-level analysis built around a human-calibrated LLM judge. Using this framework, we extend the analysis to a wider range of prior measures, including math-domain-specific diversity metrics, and show that they remain unreliable for detecting fine-grained differences in approaches. This mismatch between surface- and approach-level diversity persists in re-

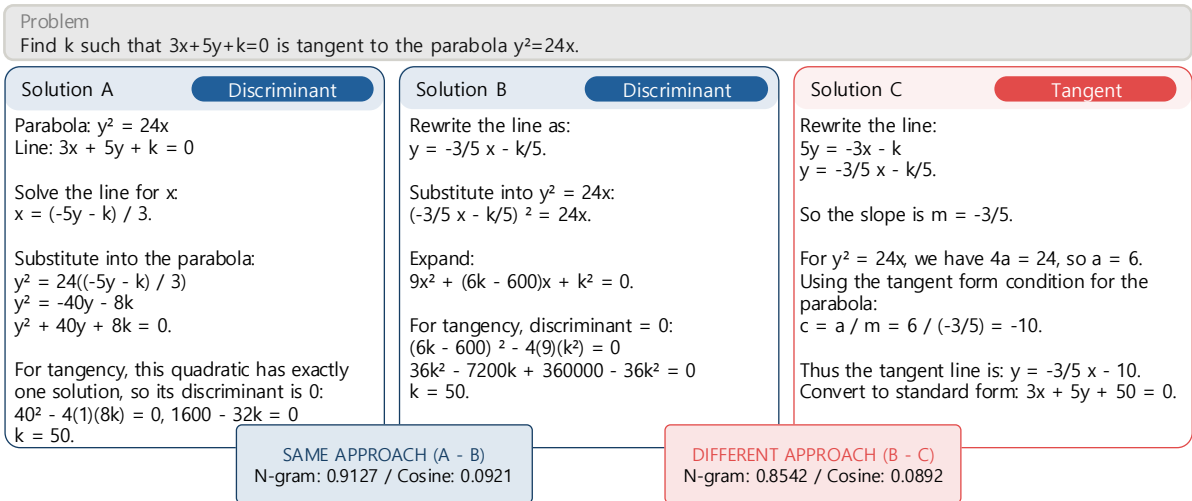


Figure 1: **A real-world failure case of conventional diversity metrics.** Conventional metrics assign a higher diversity score to a pair of solutions that follow the same approach than to a pair that uses different mathematical approaches, illustrating a mismatch between surface-level variation and approach-level diversity.

cent diversity-aware RLVR algorithms. Although these methods preserve the diversity proxies they optimize, this does not imply that approach-level diversity is preserved. In practice, training often increases surface variation within a narrower set of approaches, making outputs look more diverse even as approach-level diversity declines.

We finally ask two questions: what practical benefits approach-level diversity can provide, and whether an LLM judge approach-diversity signal that works for evaluation can also be used as a training reward. Our results reveal a gap between measuring and optimizing approach-level diversity. Candidate sets containing distinct approaches yield larger gains under test-time scaling, suggesting that approach-level diversity can improve inference-time performance. However, when directly optimized for the LLM judge approach-level diversity signal, the policy learns to satisfy the judge by exploiting its bias rather than generating genuinely diverse approaches, calling for a training-compatible, robust approach-level diversity metric.

Together, our work introduces approach-level diversity as a distinct axis for analyzing mathematical reasoning in LLMs, along with a human-calibrated framework for measuring it. Using this framework, we uncover a systematic gap between surface-level and approach-level diversity: existing metrics and diversity-aware training methods capture how solutions are written rather than how problems are solved. By discovering this gap, our work marks a step toward developing LLMs that exhibit greater strategic flexibility in mathematical reasoning.

## 2 Background

### 2.1 Related Work

**Diversity collapse in RL post-training** RL-based post-training has substantially improved the generation quality of LLMs (Schulman et al., 2017; Shao et al., 2024). Recent work, however, reports that RL post-training can reduce generation diversity, leading to narrower task coverage (Wu and Choi, 2025; Yue et al., 2025; Kirk et al., 2024; Cui et al., 2025) and more homogeneous outputs (Chen et al., 2026; Hu et al., 2026). This has motivated diversity-aware RLVR methods that aim to preserve diversity during training by adding auxiliary rewards or regularizers based on likelihood (He et al., 2025; Lanchantin et al., 2025), embedding-space distance (Chen et al., 2026, 2025), or token-level overlap (Hu et al., 2026; Lanchantin et al., 2025). Because most of these works focus on math reasoning tasks—a dominant testbed for RLVR methods—several have proposed diversity measures for mathematical reasoning to analyze such diversity collapse and guide mitigation efforts.

### Measuring diversity in mathematical reasoning

Diversity in mathematical reasoning has been measured with lexical overlap (Hu et al., 2026), symbolic proxies (Wu et al., 2024b; He et al., 2025), embedding similarity (Chen et al., 2026), and LLM-based reasoning-path decompositions (Ju et al., 2026). However, these metrics define difference through their chosen representation, leaving open whether they align with human judgments of dis-

Metric	Signal	Model-based	Structure-aware
N-gram	Lexical	✗	✗
Self-BLEU	Lexical	✗	✗
Cosine	Semantic	✓	✗
Distinct-EQ	Symbolic	✗	✓
RPD	Reasoning	✓	✓

Table 1: Taxonomy of diversity metrics analyzed.

tinct solution strategies. Although human-aligned diversity has been studied in open-ended generation (Jiang et al., 2025; Zhang et al., 2025b), it remains less explored in mathematical reasoning. Existing LLM-judge-based evaluations in this domain (Li et al., 2025; Ju et al., 2026; Zhu et al., 2026) do not explicitly define the notion of diversity they measure or validate judge decisions against human judgments. We address this gap by formalizing approach-level diversity as strategy-level variation among correct solutions and by testing whether existing diversity measures and diversity-aware RLVR methods align with this definition.

## 2.2 Diversity Metrics under Evaluation

We summarize the diversity metrics serving as baselines in our evaluation. We evaluate five diversity metrics covering lexical, semantic, symbolic, and reasoning-level signals. N-gram distance (Kondrak, 2005) and Self-BLEU (Zhu et al., 2018) measure token-level lexical overlap, while cosine distance over Qwen3-Embedding-8B (Zhang et al., 2025a) measures semantic similarity. We also include two math-specific metrics: Distinct-Equations (Wu et al., 2024b), which measures the ratio of unique equations in a solution set, and RPD (Ju et al., 2026), which decomposes solutions into reasoning steps and aggregates step-level embedding distances. Formal definitions are in Appendix B.1.

## 3 Conventional Metrics Do Not Capture Approach-level Diversity

We begin by defining the object of study: approach-level diversity in mathematical reasoning. We then construct human reference labels for this notion and use them to diagnose where representative conventional metrics fail, tracing these failures to structural properties of mathematical solutions.

### 3.1 Defining Approach-level Diversity

We define *approach-level diversity* as the variation in the underlying problem-solving strategies used

to solve the same mathematical problem correctly. This is distinct from *surface-level diversity*, which refers to the variation in the observable form of a solution, such as wording, notation, formatting, equation layout, or exposition style. Two solutions can look different while following the same strategy, or share much of their observable form while relying on different mathematical mechanisms. Approach-level diversity captures the latter distinction, which we operationalize as follows.

#### Definition of Different Approaches

We say two solutions follow different approaches if they diverge meaningfully along at least one of the following three dimensions:

- **Mathematical tools** — the techniques invoked (e.g., algebraic vs. geometric).
- **Structural definitions** — how the problem is set up (e.g., auxiliary function vs. direct substitution).
- **Representational viewpoint** — the perspective taken (e.g., coordinate vs. synthetic geometry).

### 3.2 Human Judgments of Approach Diversity

To test whether conventional diversity metrics capture approach-level diversity, we construct a human reference for metric comparisons. Following Section 3.1, annotators judge whether two correct solutions to the same problem use the same underlying approach. Our annotation set contains 80 solution pairs from 20 problems from the MATH (Hendrycks et al., 2021) training set, with four model-generated pairs per problem. Each item includes the problem and two correct model-generated solutions, and receives two independent labels from 17 annotators, each holding at least a bachelor’s degree in an engineering-related field.

Annotators agreed on 80% of the items, suggesting that the definition can be applied with reasonable consistency. The disagreements were resolved by the authors. After this, we use the resulting labels as the human reference for the analyses below. Further details are provided in Appendix E.2.

### 3.3 Failure Modes of Conventional Metrics

We compare the human labels with two representative conventional metrics: bigram distance and cosine distance. The metrics disagree with human judgments in both directions: they sometimes assign high distances to same-approach pairs and low distances to different-approach pairs. We trace this mismatch to two properties of solutions in mathematical reasoning.

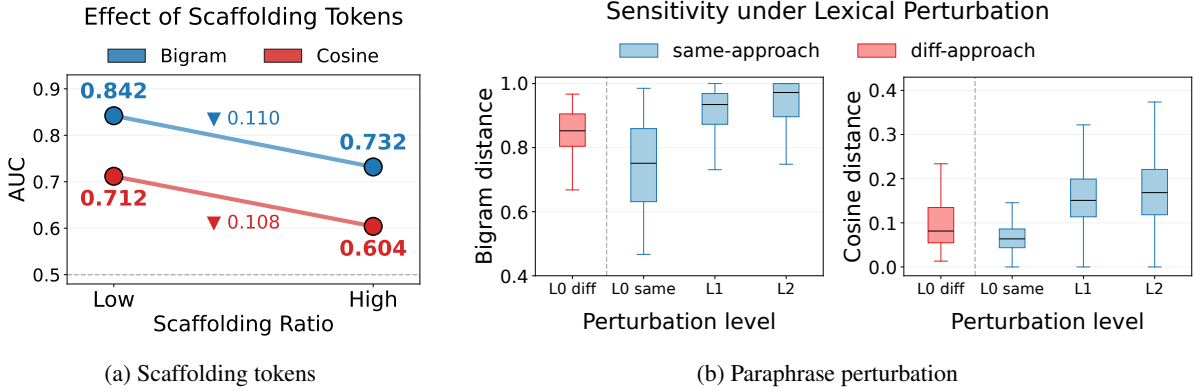


Figure 2: **Limitations of conventional diversity metrics.** (a) Conventional metrics fail to discriminate approach signals under heavy scaffolding. (b) Conventional metrics remain sensitive to realistic paraphrases.

**Two Confounds Behind the Disagreement** The disagreement stems from two factors that conventional metrics cannot separate from the actual approach. The first is *shared scaffolding*: content that most correct solutions to a problem include regardless of approach, such as restated conditions, common setup steps, and answer formatting. The second is *approach-preserving paraphrasing*: changes in wording, notation, equation arrangement, or exposition that alter how a solution looks while leaving its underlying approach unchanged.

Figure 1 illustrates a real-world example. Solutions A and B use the same discriminant-based approach but differ in local algebra, while Solutions B and C use different mechanisms but share similar notation. Thus, the metrics assign higher diversity to the same-approach pair than to the different-approach pair, reversing the human decision.

**Scaffolding Weakens Approach Signals** When solutions share substantial scaffolding, conventional metrics may struggle to isolate approach-specific signals. We test this by asking whether their discriminative ability degrades on high-scaffolding problems. For each problem in our human annotation set, we compute a scaffolding score as the ratio of overlapping unigrams among correct solutions, and split problems at the median into low- and high-overlap groups. The median overlap is 61.2%, suggesting that shared setup accounts for a large portion of solutions. As Figure 2a shows, both metrics become substantially less discriminative in the high-overlap group. This indicates that shared scaffolding can dominate solution-level similarity scores, masking the smaller portion that reflects the approach. Details of the scaffolding-ratio computation are provided in Appendix D.

**Sensitivity to Paraphrasing** Even pure rewording can prevent conventional metrics from measuring approach-specific differences. To test this, we generate approach-preserving paraphrases at two levels. Starting from each original solution (L0), L1 applies local wording or notation rewrites (e.g.,  $y = mx + b$  as  $mx - y + b = 0$ ), while L2 additionally changes the global presentation format (e.g., verbose versus compact exposition); we generate three paraphrases for each original solution.

We then compare the distance distributions of rewritten same-approach solution pairs with those of original different-approach pairs. Figure 2b shows that even L1 rewrites are enough to push same-approach pairs farther apart than different-approach pairs, and the small gap between L1 and L2 indicates that most of this distortion already arises from local rewording rather than presentation shifts. Thus, conventional metrics are vulnerable even to realistic paraphrases, reflecting how a solution is written rather than how it is solved.

## 4 Approach Mismatch Persists at Scale

The previous section showed that conventional metrics cannot reliably capture approach-level diversity, motivating an evaluation framework that looks beyond surface form. We build such a framework around an LLM judge and use it to scale our analysis to real model generations, broadening the set of metrics under study and applying the framework to recent diversity-aware RLVR methods.

### 4.1 Approach Evaluation with LLM Judge

In this section, we describe our LLM-judge-based evaluation framework and explain the design choices behind it. Implementation details are

provided in Appendix E and J. To build a robust and reliable evaluation framework, we consider the following requirements.

- **D1: Approach-feasible evaluation.** Approach-level diversity can be meaningfully evaluated only on problems that admit multiple approaches.
- **D2: Scalable and interpretable labeling.** Evaluation should scale across many problems and models while producing labels that can be reused in downstream analyses.
- **D3: Human-calibrated decision boundary.** The judge should align with human judgments, especially on clear cases where annotators agree.

We address these three requirements as follows.

**Approach-feasible problem set** First, we filter for problems that admit multiple correct approaches. For each candidate problem, we (i) prompt GPT-5.2 to generate four distinct approaches, (ii) ask Qwen3-4B to solve the problem with each one and keep only those that reach the correct answer, and (iii) use a GPT-5.2 judge to confirm that the surviving approaches are mutually distinct. We retain only problems with at least three unique and correct approaches, giving 469 problems sampled from the MATH training set (Hendrycks et al., 2021). The remaining analyses in this section are performed on this evaluation set, which we release publicly.

**Clustering with an LLM judge** To obtain scalable and reusable approach labels, we ask the judge to cluster correct solutions for each problem by their underlying approach. Given a problem  $x$  and a set of correct solutions  $S_x$ , an LLM Judge  $\mathcal{J}$  powered by GPT-5.2 partitions  $S_x$  into approach-level clusters,

$$\mathcal{J}(x, S_x) = C_1, \dots, C_{K_x}, \quad S_x = \bigsqcup_{i=1}^{K_x} C_i. \quad (1)$$

Each cluster  $C_i$  contains solutions judged to follow the same approach, and  $K_x$  denotes the number of distinct approaches identified for problem  $x$ .

**Agreement with human annotations** We validate the judge against the human labels from Section 3.2. The judge achieves 85.0% agreement with the human reference labels, comparable to the 80.0% inter-annotator agreement. Moreover, among the 64 clear cases on which all annotators agreed, the judge disagreed on only 2, indicating that the judge aligns well with human judgments.

## 4.2 Existing Measures Fail to Capture Fine-Grained Differences

Using our evaluation framework, we show that the limitations in Section 3.3 persist across a broader set of diversity measures introduced in Section 2.2: prior metrics detect whether a solution set uses one approach or many, but lose discriminative power on finer differences within approach-diverse sets.

**Concordance analysis** We evaluate each diversity metric  $D$  with a simple ranking question: given two solution sets, how often does  $D$  assign the higher score to the more approach-diverse one? We denote this measure as *concordance*. For each problem, the LLM judge first clusters correct solutions by approach. We then sample equal-sized pairs  $(S_{\text{high}}, S_{\text{low}})$  with  $|S_{\text{high}}| = |S_{\text{low}}| = k$ , where  $S_{\text{high}}$  covers more distinct approaches than  $S_{\text{low}}$ . The solutions are distributed as evenly as possible across distinct approaches. For each question, we repeat the test  $B$  times, and count how often the metric gets it right,

$$C_{\text{set}}(D) = \frac{1}{B} \sum_{b=1}^B \mathbb{1} \left[ D(S_{\text{high}}^{(b)}) > D(S_{\text{low}}^{(b)}) \right], \quad (2)$$

which is then averaged over the problems. For pairwise distance metrics,  $D(S)$  denotes the mean pairwise distance within  $S$ . Solutions are drawn from three base models: Qwen2.5-32B-Base (Team, 2024), Qwen3-8B-Base (Team, 2025), and OLMo3-32B-Base (Olmo et al., 2026). We report results with  $k = 4$  in the main text.

**From coarse to fine-grained comparisons** The easy case is when  $S_{\text{low}}$  uses just one approach, where solutions look nearly identical, so even surface-level metrics can tell them apart from a varied  $S_{\text{high}}$ . The more important question is whether a metric can detect a finer difference when  $S_{\text{low}}$  itself already induces substantial surface diversity.

To separate these cases, we use a tiered evaluation. At Tier  $n$ ,  $S_{\text{low}}$  contains solutions from  $n$  distinct approaches, while  $S_{\text{high}}$  contains  $n+1$  distinct approaches. Tier 1 then compares one approach against two, acting as a coarse contrast. Tiers 2 and 3 are stricter: they ask whether a metric can detect the incremental gain from adding one more approach to an already multi-approach set. These higher tiers test whether a metric truly captures approach-level diversity beyond surface form.

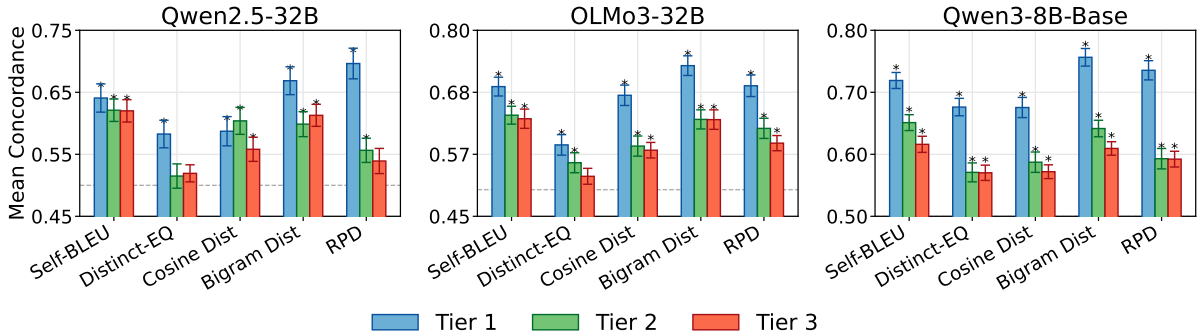


Figure 3: **Set-level concordance** ( $C_{\text{set}}$ ) at subset size  $k = 4$  across solver models. Bars show mean concordance with 95% confidence intervals. Asterisks indicate values that are significantly above the random baseline at  $p = 0.05$ .

	Qwen2.5-3B			Qwen2.5-7B		
	Quality		Diversity	Quality		Diversity
	Pass@1	Pass@32	Cov@16	Pass@1	Pass@32	Cov@16
Base	15.19	60.30	2.302	19.10	66.52	1.956
GRPO	27.81	64.44	1.786	37.08	71.70	1.761
DQO	26.48	63.85	1.853	31.86	66.20	1.508
DIVER-TD	28.22	65.93	1.519	38.36	72.19	1.524
DIVER-ED	29.31	66.67	1.884	39.42	71.11	1.573

Table 2: Quality and diversity comparison across different diversity-aware RL algorithms.

**Results** Figure 3 shows a consistent pattern across metrics and generator models. Existing metrics perform well in Tier 1, where the comparison is between a single-approach set and a multi-approach set. However, their concordance drops substantially in Tiers 2 and 3, where both sets already contain multiple approaches. Thus, prior metrics can detect coarse diversity contrasts, but struggle to resolve incremental gains in approach-level diversity once both solution sets are already diverse. Appendix F shows the same pattern under other settings.

### 4.3 What Diversity Does Diversity-Aware RLVR Preserve?

Diversity-aware RLVR methods aim to preserve generation diversity, but typically optimize surface-level measures. Given the gap between these measures and approach-level diversity, we ask whether such methods broaden the set of approaches or merely produce surface variants of the same ones. We study two recent baselines: DQO (Chen et al., 2026), which rewards embedding diversity, and DIVER (Hu et al., 2026), which combines textual diversity (TD) via pairwise BLEU with equation diversity (ED) via distinct equations. Appendix B.2 provides full descriptions.

**Measuring approach coverage** We measure approach-level diversity of a policy  $\pi$  with *expected coverage*  $\text{cov}(N, \pi)$ : the expected number of distinct approach clusters observed when sampling  $N$  correct solutions from  $\pi$ . This captures not only the number of covered approaches, but also how evenly the policy samples across them. For a problem  $x$ , we define this over sets  $S_x$  of  $N$  correct samples:

$$\text{cov}_x(N, \pi) = \mathbb{E}_{S_x} [|\mathcal{J}(x, S_x)|], \quad |S_x| = N, \quad (3)$$

where  $\mathcal{J}(x, S_x)$  is the clustering produced by the judge from Section 4.1, with estimation details deferred to Appendix G.2.

**Experimental setup** We train Qwen2.5-3B/7B-Base models on the MATH training set for 100 steps. For each trained policy, we measure quality by accuracy on OlympiadBench (He et al., 2024). For diversity, we evaluate approach coverage on 150 problems from the approach-feasible problem set in Section 4.1, retaining only those for which every Qwen2.5-3B checkpoint, including the base model, produces at least 16 correct solutions. This restriction ensures that coverage is estimated from enough correct samples for a reliable comparison.

**Results** Table 2 shows that approach-level diversity declines after RLVR across all settings, indicating that RLVR’s diversity decline also appears at the approach level. Moreover, preserving the optimized proxy does not imply preserving approach-level diversity: DIVER maintains its textual or equation-level diversity signals during training (Figure 4a), but still loses approach coverage.

To understand what these targeted gains represent, we decompose DIVER’s target-metric improvements between steps 25 and 100, where the optimized metrics increase. The decomposi-

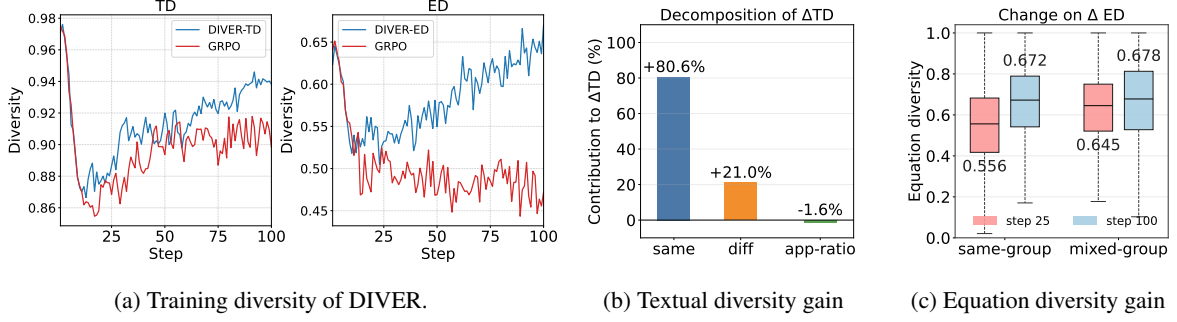


Figure 4: **Analysis of DIVER.** DIVER preserves its target TD and ED metrics, but the recovered diversity mostly reflects within-approach variation rather than broader approach coverage. See Appendix G.4 for details.

tion shows that the gains come mainly from making solutions within the same approach more varied, rather than from producing more diverse approaches. In Figure 4b, 80.6% of the textual diversity gain comes from greater variation among same-approach pairs. Figure 4c shows a similar pattern for equations: same-approach equation diversity rises sharply, while cross-approach equation diversity remains relatively consistent.

These results reveal a key implication: optimizing surface-level diversity can make generations look more diverse without widening the set of strategies the policy uses. Instead, it produces more varied realizations of a narrower set of reasoning strategies. Further details are in Appendix G.

## 5 The Utility and Limits of Optimizing Approach-Level Diversity

Having shown that conventional metrics misalign with approach-level diversity, we now ask two questions: does approach-level diversity help downstream performance, and can we induce it directly? We address the first through approach-controlled test-time scaling, and the second through reward optimization with an LLM judge.

### 5.1 Approach diversity for Test-Time Scaling

We first test whether approach-level diversity improves test-time scaling. Given equally sized candidate sets that differ only in the number of covered approaches, we compare three representative scaling methods: self-consistency (Wang et al., 2023), best-of- $N$  (Lightman et al., 2023), and pass@k, using a setup inspired by Handa et al. (2026).

**Approach-controlled subsets** For this experiment, we use the approach-feasible set from Section 4.1, where  $x$  is associated with valid and distinct approach plans  $C = \{c_1, \dots, c_K\}$ . For each

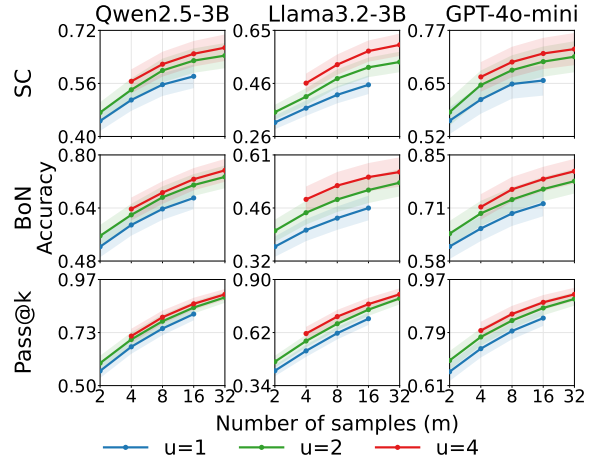


Figure 5: **Approach-controlled test-time scaling** with varying numbers of unique approaches. 95% confidence intervals are computed across problems.

plan  $c_k$ , we prompt a solver model  $p_\theta$  to generate  $R$  independent solutions,

$$S = \bigcup_{k=1}^K S_k, \quad S_k = \{s_{kj} \sim p_\theta(\cdot | x, c_k)\}_{j=1}^R.$$

We then form subsets  $\tilde{S}_{m,u} \subset S$ , where  $m$  is the total number of solutions and  $u$  is the number of covered approaches. For fixed  $m$ , we vary  $u$  by sampling  $u$  approach plans and drawing  $m/u$  solutions from each. By construction, the expected single-solution quality is the same among subsets, so higher performance after test-time scaling directly indicates higher gains.

**Results** Across three model families, Qwen2.5-3B-Instruct (Team, 2024), Llama3.2-3B-Instruct (AI@Meta, 2024), and GPT-4o-mini (OpenAI, 2024), Figure 5 shows a consistent trend: covering more approaches improves test-time scaling at the same sampling budget, suggesting that approach-level diversity provides utility at inference time.

	Quality		Diversity
	Pass@1	Pass@32	Cov@16
GRPO	27.81	64.44	1.786
DIVER-Judge	29.70	65.00	1.426

Table 3: Results of training with LLM-judge-based diversity reward under DIVER framework.

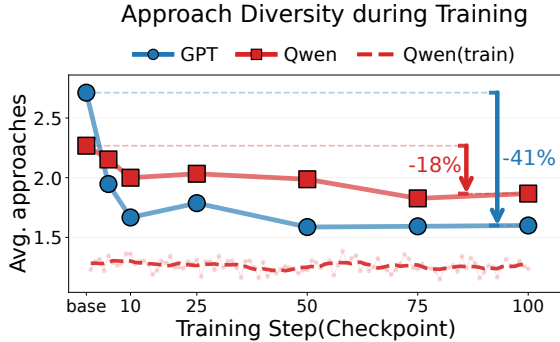


Figure 6: **Solid lines**: average number of unique approaches per problem on eval set, by the training judge (Qwen, red) and an external GPT judge (blue). **Dashed line**: in-batch training diversity scored by the Qwen judge. More results can be found in Appendix H.2.

## 5.2 Optimizing an LLM Judge Reward Amplifies Judge Bias

We next ask whether approach-level diversity can be directly encouraged during training through an LLM-judge-based reward. Section 4.3 showed that surface-level rewards maintain their target proxies but that approach-level diversity declines. A natural question is to reward approach-level diversity directly, using an LLM-judge-based reward. We instantiate this with a 35B open-source judge, but find that direct optimization fails in a different way: the policy learns judge-specific preferences rather than broadening its set of approaches.

**Setup** We reuse the judging procedure from Section 4.1, changing only the backbone to Qwen3.5-35B-A3B (Team, 2026) due to training cost. Given a problem and the correct rollouts in a training batch, the judge clusters them into approaches as in Equation 1. Each correct rollout  $s_i \in C_j$  receives a diversity reward  $r_{\text{div}} = 1/\sqrt{|C_j|}$ , giving higher reward to rollouts from smaller approach clusters. Also, for a fixed number of approaches, the reward is maximized when rollouts are balanced across approaches, matching the expected-coverage criterion used in our evaluation. We plug this reward into DIVER, keep the remaining training setup from Section 4.3, and train Qwen2.5-3B on MATH.

**Results** Despite optimizing an explicit approach-diversity reward, the judge-reward checkpoint becomes less diverse than naive GRPO (Table 3), suggesting reward hacking against the in-loop judge (Qwen). Figure 6 compares its judged diversity with that from a held-out, human-calibrated judge (GPT). The two flip their ordering across training: before training, the held-out judge rates rollouts as more diverse, but after training, this ordering reverses. This rules out the held-out judge simply being stricter, and matches the canonical signature of reward hacking—the policy learns judge-specific preferences rather than broadening its solution strategies. Naive use of an LLM judge thus does not cleanly transfer diversity from evaluation to training, pointing to an open challenge: designing approach-level diversity signals that capture genuine strategy-level differences and remain robust to reward hacking when optimized against.

## 6 Discussions

**Future Research Directions** Our results suggest two directions for future work. First, useful diversity is likely to become increasingly *domain-specific* as LLMs are applied to more complex tasks. While mathematical reasoning offers a controlled setting, domains such as scientific discovery, program synthesis, and open-ended planning may demand different notions of strategic variation, motivating domain-aware definitions and evaluations of approach diversity. Second, approach-level diversity can be further studied as a *training objective*. Our evaluation framework makes it possible to identify and analyze approach-level variation at scale, opening a path toward diversity-aware optimization. The key challenge is designing objectives that preserve the human-relevant structure of approach-level diversity while remaining robust under direct optimization—a step toward training methods that encourage genuinely distinct reasoning rather than surface-level variation.

**Conclusion** We introduce approach-level diversity as a distinct axis for analyzing mathematical reasoning in LLMs. Our results show that existing metrics and diversity-aware training methods often conflate surface variation with genuinely distinct solution strategies. By making this gap explicit, we believe our analysis points toward training and evaluation that better reflect human-aligned notions of diversity in mathematical reasoning.

## Limitations

**Focus on Mathematical Reasoning** We focus on mathematical reasoning because the distinction between surface form and approach-level structure is relatively clear, and because recent diversity-aware RLVR methods are largely studied on math benchmarks. A natural next step is to extend this analysis to domains where higher-level strategic diversity may provide more direct benefits, such as program synthesis, scientific discovery, or open-ended planning.

**Non-exhaustive Coverage** We evaluate representative diversity metrics and recent diversity-aware RLVR methods, but do not exhaustively cover all possible metrics, training objectives, or decoding strategies. Our results should therefore be read as evidence of a mismatch in commonly used diversity proxies, rather than as an exhaustive survey of diversity methods.

**No General Mitigation Method** Our work identifies and analyzes the mismatch between diversity proxies and approach diversity, but does not provide a general method for preserving or inducing approach diversity during training. Future work may require both more faithful reward signals and training algorithms that can optimize them without proxy exploitation.

## References

AI@Meta. 2024. [Llama 3 model card](#).

Jianlv Chen, Shitao Xiao, Peitian Zhang, Kun Luo, Defu Lian, and Zheng Liu. 2024. [Bge m3-embedding: Multi-lingual, multi-functionality, multi-granularity text embeddings through self-knowledge distillation](#). *Preprint*, arXiv:2402.03216.

Xiwen Chen, Wenhui Zhu, Peijie Qiu, Xuanzhao Dong, Hao Wang, Haiyu Wu, Huayu Li, Aristeidis Sotiras, Yalin Wang, and Abolfazl Razi. 2025. [Dra-grpo: Exploring diversity-aware reward adjustment for rl-zero-like training of large language models](#). *arXiv preprint arXiv:2505.09655*.

Yilei Chen, Souradip Chakraborty, Lorenz Wolf, Yannis Paschalidis, and Aldo Pacchiano. 2026. [Post-training large language models for diverse high-quality responses](#). In *The Fourteenth International Conference on Learning Representations*.

Ganqu Cui, Yuchen Zhang, Jiacheng Chen, Lifan Yuan, Zhi Wang, Yuxin Zuo, Haozhan Li, Yuchen Fan, Huayu Chen, Weize Chen, and 1 others. 2025. [The entropy mechanism of reinforcement learning for reasoning language models](#).

Carlos Gómez-Rodríguez and Paul Williams. 2023. [A confederacy of models: a comprehensive evaluation of LLMs on creative writing](#). In *Findings of the Association for Computational Linguistics: EMNLP 2023*, Singapore. Association for Computational Linguistics.

Michael Günther, Jackmin Ong, Isabelle Mohr, Alaeddine Abdesslem, Tanguy Abel, Mohammad Kalim Akram, Susana Guzman, Georgios Mastrapas, Saba Sturua, Bo Wang, Maximilian Werk, Nan Wang, and Han Xiao. 2024. [Jina embeddings 2: 8192-token general-purpose text embeddings for long documents](#). *Preprint*, arXiv:2310.19923.

Divij Handa, Mihir Parmar, Aswin RRV, Md Nayem Uddin, Hamid Palangi, and Chitta Baral. 2026. [Guidedsampling: Steering llms towards diverse candidate solutions at inference-time](#). *Preprint*, arXiv:2510.03777.

Andre Wang He, Daniel Fried, and Sean Welleck. 2025. [Rewarding the unlikely: Lifting grpo beyond distribution sharpening](#). In *Proceedings of the 2025 Conference on Empirical Methods in Natural Language Processing*, pages 25559–25571.

Chaoqun He, Renjie Luo, Yuzhuo Bai, Shengding Hu, Zhen Thai, Junhao Shen, Jinyi Hu, Xu Han, Yujie Huang, Yuxiang Zhang, and 1 others. 2024. [Olympiadbench: A challenging benchmark for promoting agi with olympiad-level bilingual multimodal scientific problems](#). In *Proceedings of the 62nd Annual Meeting of the Association for Computational Linguistics (Volume 1: Long Papers)*, pages 3828–3850.

Dan Hendrycks, Collin Burns, Saurav Kadavath, Akul Arora, Steven Basart, Eric Tang, Dawn Song, and Jacob Steinhardt. 2021. [Measuring mathematical problem solving with the math dataset](#). *arXiv preprint arXiv:2103.03874*.

Zican Hu, Shilin Zhang, Yafu Li, Jianhao Yan, Xuyang Hu, Leyang Cui, Xiaoye Qu, Chunlin Chen, Yu Cheng, and Zhi Wang. 2026. [Diversity-incentivized exploration for versatile reasoning](#). In *The Fourteenth International Conference on Learning Representations*.

Liwei Jiang, Yuanjun Chai, Margaret Li, Mickel Liu, Raymond Fok, Nouha Dziri, Yulia Tsvetkov, Maarten Sap, Alon Albalak, and Yejin Choi. 2025. [Artificial hivemind: The open-ended homogeneity of language models \(and beyond\)](#). *Preprint*, arXiv:2510.22954.

Feng Ju, Zeyu Qin, Rui Min, Zhitao He, Lingpeng Kong, and Yi R. Fung. 2026. [Reasoning path divergence: A new metric and curation strategy to unlock llm diverse thinking](#). *Preprint*, arXiv:2510.26122.

Robert Kirk, Ishita Mediratta, Christoforos Nalmpantis, Jelena Luketina, Eric Hambro, Edward Grefenstette, and Roberta Raileanu. 2024. [Understanding the effects of rlhf on llm generalisation and diversity](#). In *The Twelfth International Conference on Learning Representations*.

- Grzegorz Kondrak. 2005. N-gram similarity and distance. In *International symposium on string processing and information retrieval*, pages 115–126. Springer.
- Woosuk Kwon, Zhuohan Li, Siyuan Zhuang, Ying Sheng, Lianmin Zheng, Cody Hao Yu, Joseph Gonzalez, Hao Zhang, and Ion Stoica. 2023. [Efficient memory management for large language model serving with pagedattention](#). In *Proceedings of the 29th Symposium on Operating Systems Principles, SOSP '23*, page 611–626, New York, NY, USA. Association for Computing Machinery.
- Jack Lanchantin, Angelica Chen, Shehzaad Dhuliawala, Ping Yu, Jason Weston, Sainbayar Sukhbaatar, and Ilya Kulikov. 2025. Diverse preference optimization. *arXiv preprint arXiv:2501.18101*.
- Tianjian Li, Yiming Zhang, Ping Yu, Swarnadeep Saha, Daniel Khashabi, Jason Weston, Jack Lanchantin, and Tianlu Wang. 2025. Jointly reinforcing diversity and quality in language model generations. *arXiv preprint arXiv:2509.02534*.
- Hunter Lightman, Vineet Kosaraju, Yura Burda, Harri Edwards, Bowen Baker, Teddy Lee, Jan Leike, John Schulman, Ilya Sutskever, and Karl Cobbe. 2023. [Let’s verify step by step](#). *Preprint*, arXiv:2305.20050.
- Team Olmo, :, Allyson Ettinger, Amanda Bertsch, Bailey Kuehl, David Graham, David Heineman, Dirk Groeneveld, Faeze Brahman, Finbarr Timbers, Hamish Ivison, Jacob Morrison, Jake Poznanski, Kyle Lo, Luca Soldaini, Matt Jordan, Mayee Chen, Michael Noukhovitch, Nathan Lambert, and 50 others. 2026. [Olmo 3](#). *Preprint*, arXiv:2512.13961.
- OpenAI. 2024. [Hello gpt-4o](#).
- OpenAI. 2024. New embedding models and API updates. <https://openai.com/index/new-embedding-models-and-api-updates/>. Accessed: 2026-05-26.
- OpenAI. 2026. Introducing GPT-5.4 mini and nano. <https://openai.com/index/introducing-gpt-5-4-mini-and-nano/>. Accessed: 2026-05-26.
- Isha Puri, Mehul Damani, Idan Shenfeld, Marzyeh Ghassemi, Jacob Andreas, and Yoon Kim. 2026. [Reaching beyond the mode: RL for distributional reasoning in language models](#). *Preprint*, arXiv:2603.24844.
- John Schulman, Filip Wolski, Prafulla Dhariwal, Alec Radford, and Oleg Klimov. 2017. [Proximal policy optimization algorithms](#). *Preprint*, arXiv:1707.06347.
- Zhihong Shao, Peiyi Wang, Qihao Zhu, Runxin Xu, Junxiao Song, Xiao Bi, Haowei Zhang, Mingchuan Zhang, YK Li, and 1 others. 2024. Deepseekmath: Pushing the limits of mathematical reasoning in open language models. *arXiv preprint arXiv:2402.03300*.
- Guangming Sheng, Chi Zhang, Zilingfeng Ye, Xibin Wu, Wang Zhang, Ru Zhang, Yanghua Peng, Haibin Lin, and Chuan Wu. 2024. Hybridflow: A flexible and efficient rlhf framework. *arXiv preprint arXiv:2409.19256*.
- Ilya Shumailov, Zakhar Shumaylov, Yiren Zhao, Nicolas Papernot, Ross Anderson, and Yarin Gal. 2024. [AI models collapse when trained on recursively generated data](#). *Nature*, 631(8022):755–759.
- Tarun Suresh, Revanth Gangi Reddy, Yifei Xu, Zach Nussbaum, Andriy Mulyar, Brandon Duderstadt, and Heng Ji. 2025. [Cornstack: High-quality contrastive data for better code retrieval and reranking](#). *Preprint*, arXiv:2412.01007.
- Qwen Team. 2024. [Qwen2.5: A party of foundation models](#).
- Qwen Team. 2025. [Qwen3 technical report](#). *Preprint*, arXiv:2505.09388.
- Qwen Team. 2026. [Qwen3.5: Accelerating productivity with native multimodal agents](#).
- Xuezhi Wang, Jason Wei, Dale Schuurmans, Quoc V Le, Ed H Chi, Sharan Narang, Aakanksha Chowdhery, and Denny Zhou. 2023. Self-consistency improves chain of thought reasoning in language models. In *The Eleventh International Conference on Learning Representations*.
- Fang Wu and Yejin Choi. 2025. The invisible leash: Why rlvr may not escape its origin. In *2nd AI for Math Workshop@ ICML 2025*.
- Qingyun Wu, Gagan Bansal, Jieyu Zhang, Yiran Wu, Beibin Li, Erkang Zhu, Li Jiang, Xiaoyun Zhang, Shaokun Zhang, Jiale Liu, and 1 others. 2024a. Autogen: Enabling next-gen llm applications via multi-agent conversations. In *First Conference on language modeling*.
- Ting Wu, Xuefeng Li, and Pengfei Liu. 2024b. Progress or regress? self-improvement reversal in post-training. In *The Thirteenth International Conference on Learning Representations*.
- Yang Yue, Zhiqi Chen, Rui Lu, Andrew Zhao, Zhaokai Wang, Shiji Song, and Gao Huang. 2025. Does reinforcement learning really incentivize reasoning capacity in llms beyond the base model?
- Yanzhao Zhang, Mingxin Li, Dingkun Long, Xin Zhang, Huan Lin, Baosong Yang, Pengjun Xie, An Yang, Dayiheng Liu, Junyang Lin, Fei Huang, and Jingren Zhou. 2025a. [Qwen3 embedding: Advancing text embedding and reranking through foundation models](#). *Preprint*, arXiv:2506.05176.
- Yiming Zhang, Harshita Diddee, Susan Holm, Hanchen Liu, Xinyue Liu, Vinay Samuel, Barry Wang, and Daphne Ippolito. 2025b. Noveltybench: Evaluating language models for humanlike diversity. In *Conference on Language Modeling (COLM)*.

Zhenru Zhang, Chujie Zheng, Yangzhen Wu, Beichen Zhang, Runji Lin, Bowen Yu, Dayiheng Liu, Jingren Zhou, and Junyang Lin. 2025c. [The lessons of developing process reward models in mathematical reasoning](#). In *Findings of the Association for Computational Linguistics: ACL 2025*, pages 10495–10516, Vienna, Austria. Association for Computational Linguistics.

Xuekai Zhu, Daixuan Cheng, Dinghui Zhang, Hengli Li, Kaiyan Zhang, Che Jiang, Youbang Sun, Ermo Hua, Yuxin Zuo, Xingtai Lv, and 1 others. 2026. [FlowRL: Matching reward distributions for LLM reasoning](#). In *The Fourteenth International Conference on Learning Representations*.

Yaoming Zhu, Sidi Lu, Lei Zheng, Jiaxian Guo, Weinan Zhang, Jun Wang, and Yong Yu. 2018. [Taxygen: A benchmarking platform for text generation models](#). In *The 41st international ACM SIGIR conference on research & development in information retrieval*, pages 1097–1100.

## A Common Experimental Details

**Sampling prompt** Unless otherwise specified, we use the sampling prompt in Figure 7 for all solution generation. This includes both offline solution generation for analysis and rollout sampling during RLVR training and evaluation.

**Answer verification** We verify final-answer correctness using Qwen3-4B with the prompt in Figure 8. For each generated solution, we extract the predicted answer from the `\boxed{}` expression; if no boxed answer is found, we use the last 300 characters of the solution instead. The verifier is then given the predicted answer and the ground-truth answer, and is instructed to output either correct or incorrect.

We use a judge-based verifier because it is more robust than rule-based matching for general mathematical answers, where equivalent answers may be written in different forms.

**Base Sampling Prompt**

```

### Problem: {problem}
Please reason step by step, and put your answer within \boxed{}
### Solution:

```

Figure 7: Solution generation prompt.

**Answer Verification Prompt**

```

System message:
You are a math expert.
You are given a golden answer and a predicted answer from a solver.

```

```

You need to verify if the predicted answer is correct.
Only output "correct" or "incorrect".

Few-shot messages:
User:
Golden answer: 540, Predicted answer: The total number of ways the cars can stack up so that all three lanes are occupied is calculated to be 750.

Assistant:
incorrect

User:
Golden answer: 3, Predicted answer: The ratio \frac{AC}{AE} = 3.

Assistant:
correct

Query message:
User:
Golden answer: {golden_answer}, Predicted answer: {predicted_answer}

Output constraint:
Assistant:
correct
or
incorrect

```

Figure 8: Answer verification prompt. The model is instructed to determine whether a predicted answer matches the golden answer, using few-shot examples and constrained to output either “correct” or “incorrect”.

## B Detailed Background on Diversity Metrics and Diversity-Aware RLVR

### B.1 Diversity Metrics under Analysis

Full list of analyzed diversity metrics and their detailed definitions are listed below:

- **Cosine Embedding** given two solutions  $s_A$ ,  $s_B$ , and an embedding model  $E$ , the distance between the two solutions is calculated as  $d(s_A, s_B) = 1 - \frac{E(s_A) \cdot E(s_B)}{\|E(s_A)\| \cdot \|E(s_B)\|}$
- **Self-BLEU** Proposed by [Zhu et al. \(2018\)](#), Self-BLEU measures lexical homogeneity by treating each solution as a hypothesis against the rest as references:

$$\text{Self-BLEU}(S) = \frac{1}{N} \sum_{i=1}^N \text{BLEU}(s_i, S \setminus \{s_i\}).$$

We report  $1 - \text{Self-BLEU}(S)$ .

- **N-gram Distance** Given the  $n$ -gram multisets  $G_n(s_A)$  and  $G_n(s_B)$ , the pairwise distance is defined as the Jaccard distance:

$$d_n(s_A, s_B) = 1 - \frac{|G_n(s_A) \cap G_n(s_B)|}{|G_n(s_A) \cup G_n(s_B)|}.$$

Our main analysis uses  $n = 2$ . Ablations for different values of  $n$  can be found in Appendix F

- **Distinct-Equations** (Distinct-EQ) Wu et al. (2024b) The calculation of this metric is done in two steps: extracting equations from the input solution set and computing the ratio of unique equations. Let  $\text{Eq}(S)$  denote the multiset of all extracted equations from  $S$ . Then:

$$D_{\text{eq}}(S) = \frac{|\text{Unique}(\text{Eq}(S))|}{|\text{Eq}(S)|}$$

- **RPD** Suggested by Ju et al. (2026), this metric aims to discriminate between two solutions for a math problem by their reasoning trajectory. Given two solutions  $s_A$  and  $s_B$ , it first extracts step-level representations using an LLM:  $L_A = a_1, a_2, \dots, a_m$ ,  $L_B = b_1, b_2, \dots, b_n$ . Each representation is then encoded into an embedding vector, yielding a step-level distance:

$$d_i = \min_{j=1, \dots, n} \left( 1 - \frac{e_{a_i} \cdot e_{b_j}}{\|e_{a_i}\| \cdot \|e_{b_j}\|} \right)$$

The overall distance is calculated as the average of step-level distances

$$d(s_A, s_B) = \frac{1}{m} \sum_{i=1}^m d_i$$

## B.2 Diversity-Aware RLVR Baselines

**DQO.** DQO (Chen et al., 2026) adds a group-level semantic diversity objective to RL post-training. For a prompt  $x$ , let  $Y = \{y_1, \dots, y_G\}$  be a group of responses and let  $z_i = E(y_i)$  be the embedding of response  $y_i$ . DQO computes an embedding-similarity matrix  $M(Y)$  over the group and uses its determinant as the diversity signal:

$$D_{\text{DQO}}(Y) = \log \det(M(Y) + \epsilon I).$$

The objective can be summarized as

$$\mathcal{J}_{\text{DQO}}(\theta) = \mathbb{E}_{Y \sim \pi_\theta(\cdot|x)} [R(Y) + \alpha D_{\text{DQO}}(Y)],$$

where  $R(Y)$  denotes the quality reward and  $\alpha$  controls the strength of the diversity objective.

**DIVER.** DIVER (Hu et al., 2026) adds an intrinsic diversity reward to the verifiable reward in RLVR. Given a group of rollouts  $Y = \{y_1, \dots, y_G\}$ , each correct rollout receives a diversity bonus based on its dissimilarity to the other rollouts:

$$\tilde{r}(x, y_i) = r_{\text{ver}}(x, y_i) + \beta \mathbf{1}\{r_{\text{ver}}(x, y_i) = 1\} D_i(Y),$$

where  $r_{\text{ver}}$  is the correctness reward and  $\beta$  controls the diversity strength.

We experiment with two conventional diversity measures introduced in DIVER. Textual diversity (TD) computes  $D_i(Y)$  from pairwise BLEU:

$$D_i^{\text{TD}}(Y) = \frac{1}{G-1} \sum_{j \neq i} (1 - \text{BLEU}(y_i, y_j)).$$

Equation Diversity (ED) computes  $D_i(Y)$  with the ratio of distinct equations:

$$D_i^{\text{ED}}(Y) = \frac{|\text{Eq}(y_i) \setminus \bigcup_{j \neq i} \text{Eq}(y_j)|}{\max\{|\text{Eq}(y_i)|, 1\}}.$$

## C Additional Analysis:

### Approach-Seeking Sequential SFT

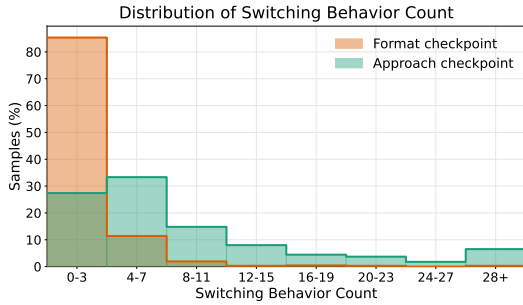
While the main paper focuses on measuring approach-level diversity, we also explore a complementary question: can encouraging a model to seek diverse approaches improve its reasoning? We compare two supervised fine-tuning datasets that share output structure but differ in approach-seeking: approach asks for three distinct mathematical approaches, while format asks for three format variants of a single approach.

### C.1 Dataset Generation

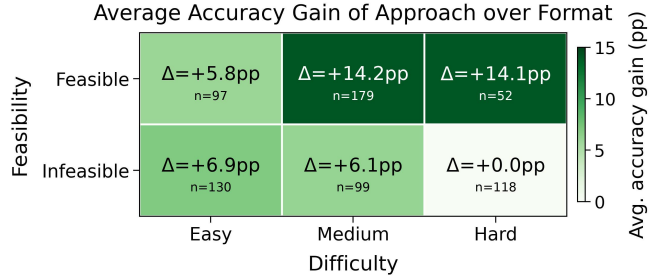
We adopt a sequential-solution generation setup inspired by Puri et al. (2026), in which a model generates multiple solutions in a single response. Both datasets are generated by Qwen3-14B and used to fine-tune Qwen3-4B, differing only in the generation prompt (Figures 18 and 19). Starting from 2,000 problems in the training set of Appendix E.1, we generate one response under each prompt and retain only problems for which all three solutions are correct in both responses.

### C.2 Behavioral and Ability Checks

We verify that the checkpoints differ in the intended behavior and not in underlying reasoning ability. For behavior, we count common approach-switching cues such as ‘‘another approach’’ and



(a) Switching-cue distribution.



(b) Gain by problem subset.

Figure 9: **Additional analysis of approach-seeking behavior.** (a) Distribution of approach-switching cues in the Format and Approach checkpoints. (b) Average accuracy gain of Approach over Format across difficulty and multi-approach feasibility partitions. Difficulty is defined by the number of correct solutions among 8 rollouts of Qwen3-4B with thinking disabled: easy = 8, medium = 1–7, and hard = 0. Multi-approach feasibility is determined using the pipeline introduced in Section 4.1.

	OlympiadBench		AIME	
	avg@3	pass@3	avg@3	pass@3
Format	55.51	65.78	47.78	58.33
Approach	67.56	69.78	50.00	56.67

Table 4: **Downstream performance of the approach-trained checkpoint.** We compare the Format and Approach checkpoints on OlympiadBench and AIME24/25. *avg@3* is the average accuracy over the three solutions in a response, while *pass@3* is the fraction of problems where at least one solution is correct.

Metric	Approach	Format
Accuracy	69.04	68.30
Freq. of approach cues	3.10	2.18

Table 5: **Results with base prompt.** Comparison between approach and format checkpoints, using the base prompt in Figure 7.

Problem subset	$\Delta$ Acc. (pp)	95% CI (pp)
Reachable	11.69	[7.32, 16.06]
Unreachable	3.50	[-0.42, 7.50]

Table 6: **Accuracy gains by approach reachability.** We report accuracy improvements of approach checkpoint over format, with 95% confidence intervals shown in brackets.

“another method” (full list in Figure 10). Figure 9a shows that the Approach checkpoint uses these cues substantially more than the Format checkpoint. For ability, we compare accuracies under the standard single-solution prompt (Figure 7): the two checkpoints achieve 69.04% (approach) and 68.30% (format), confirming that they are matched in baseline reasoning (Table 5).

**Results** Table 4 shows that the Approach checkpoint outperforms the Format checkpoint on both OlympiadBench and AIME, suggesting that approach-seeking behavior can improve accuracy in the sequential-solution setting. The per-problem breakdown in Figure 9b further shows that gains concentrate on problems with multiple approaches, and within this subset grow with difficulty.

**Reachability of an approach matters** A natural question is whether merely having multiple valid approaches is enough, or whether the target model must also be able to reach them. Our main labels conflate these factors: Qwen3-4B serves as both the correctness validator and the fine-tuned model. To decouple them, we re-run the filtering pipeline

with a stronger validator, GPT-5.4-mini (OpenAI, 2026), sampling one solution per candidate approach. This yields 30 problems that are multi-approach feasible for the stronger validator but unreachable under Qwen3-4B validation. On these problems, the Approach checkpoint improves over Format by only 3.50 percentage points (95% CI includes zero), compared with 11.69 points on reachable problems. Approach-seeking supervision thus helps only when the alternative approaches are accessible to the target model.

Approach Seeking Cues
another approach / another way
another method / different approach
first approach / second approach / third approach
let me check another way

Figure 10: Linguistic markers of approach switching.

## D Computing Scaffolding Ratio

We measure shared scaffolding with a soft unigram-overlap ratio. For each problem  $x$ , let  $S_x = \{s_1, \dots, s_n\}$  be all correct solutions. We lower-case each solution and tokenize it by whitespace. For each token  $w$ , we first compute its prevalence across correct solutions:

$$p_x(w) = \frac{1}{n} \sum_{i=1}^n \mathbf{1}[w \in U_i],$$

where  $U_i$  is the set of unique tokens in solution  $s_i$ . The scaffolding ratio of a solution is then the average prevalence of its tokens:

$$r(s_i) = \frac{1}{|T_i|} \sum_{w \in T_i} p_x(w),$$

where  $T_i$  is the token sequence of  $s_i$ . Finally, the problem-level scaffolding ratio is

$$\text{Scaffold}(x) = \frac{1}{n} \sum_{i=1}^n r(s_i).$$

This score is high when a large fraction of solution tokens also appear in many other correct solutions to the same problem, capturing shared setup, repeated notation, restated conditions, and answer-formatting patterns.

## E Approach-Level Evaluation Framework

### E.1 Details in Dataset Construction

For the main analysis in the paper, we selected problems guaranteed to have multiple solution approaches. This was done because we observed that the number of unique valid approaches to solving the problem was often constrained by the problem itself, e.g., when it is too simple or, conversely, very difficult. To this end, we introduce a four-stage filtering pipeline.

1. **Difficulty Filtering:** Given a problem  $x$ , we generate 16 solutions using the Qwen3-4B model. In this step, we filter out problems with a pass rate below 0.2 and problems with an average solution length lower than 300 tokens. By this stage, we aim to filter out problems that are either too simple or, conversely, too difficult to produce reachable, valid approaches.

2. **Plan Generation:** Given a problem  $x$ , we prompt the GPT-5.2 model to generate four distinct candidate approaches,  $C = \{c_1, c_2, c_3, c_4\}$ . For this, we used the prompt in Figure 20.
3. **Correctness Validation:** For each  $c \in C$ , we prompt a smaller language model  $\theta_{\text{solve}}$  to generate  $N = 8$  solutions from the conditioned distribution  $p_{\theta_{\text{solve}}}(\cdot|x, c)$ . We retain only those plans that yield at least one correct solution. By this, we aim to ensure both the correctness and ‘reachability’ of a specific approach - not only validating that this approach can lead to a correct answer, but also whether medium-sized language models, our primary generators in this paper, will be able to exploit such an approach effectively.
4. **Distinctness Judge:** Among the filtered plans, the GPT-5.2 judge assesses whether the surviving plans constitute meaningfully distinct approaches, and problems with fewer than three such approaches are excluded. When tested on 50 validation problems with human labels, the LLM judge reported a precision of 0.9644, a recall of 0.8714, and an F1 score of 0.9156 across 5 independent runs.

We used the GPT-5.2 model for the concept generator  $\theta_{\text{gen}}$  and uniqueness judge  $\mathcal{J}$ , and the Qwen3-4B model with thinking mode as  $\theta_{\text{solve}}$ . When applied to the MATH training dataset, this yields a training set of 2000 problems and an evaluation set of 469 problems; all analyses are conducted on the evaluation set unless otherwise specified.

### E.2 Constructing Human Annotation Set

Candidate problems were drawn from the multi-approach problem set of Section 4.1. For each candidate, we generated 32 solutions per problem from each of three base models: Qwen3-8B-Base, Qwen2.5-32B-Base, and OLMo3-32B-Base.

We then constructed annotation items in two steps. First, we manually filtered the generated solutions, keeping only those correct in both the final answer and the intermediate reasoning. Second, for each problem, the authors inspected the remaining solutions and assigned approach labels, retaining the problem only if two same-approach pairs and two different-approach pairs could be formed from a single model’s solutions. These author-provided

labels were used solely to balance the annotation set and were not shown to annotators.

Annotators were recruited from graduate students and participated voluntarily without monetary compensation. Before annotation, they were informed that their labels would be used for ML/NLP research on evaluating diversity in LLM-generated mathematical reasoning. The exact instruction is shown in Figure 11.

### E.3 Details of the LLM Judge Prompt

This section provides the full prompt template used for the LLM judge in Section 4.1, and explains the design principles behind it.

**Prompt design principles.** The prompt was designed to enforce a conservative decision boundary. First, it explicitly defines different approaches in terms of their underlying mathematical mechanisms and conceptual interpretations. Second, it instructs the judge to merge solutions when a distinction is ambiguous, weakly supported, or mainly about presentation. Third, it requires reusable outputs for downstream analysis.

In preliminary trials, we found that naively prompting the judge to cluster different approaches often led to over-splitting: solutions using the same mathematical idea were sometimes separated due to notation, formatting, verification steps, or equivalent reformulations. The final prompt, therefore, includes an explicit negative list of surface-level differences that should not define a new approach, as well as a final verification step that asks the judge to merge groups that differ only in execution details. Overall, the prompt separates solutions only when their main mathematical mechanism, structural definitions, or representational viewpoint clearly differs; otherwise, it merges solutions that differ only in presentation. All analyses were performed using the OpenAI Batch API with default sampling parameters. We set the reasoning effort to None, as we observed minimal performance gain with more reasoning budget.

**Prompt development** We developed the judge prompt using a separate validation set with only author-provided labels, constructed independently of the human annotation set in Section 3.2. The human annotation set was not used during prompt development and was reserved only for the final alignment evaluation.

Tier	$k$	Qwen2.5-32B	Qwen3-8B	OLMo3-32B
Tier 1	4	102	178	130
Tier 1	6	59	131	93
Tier 2	4	92	112	96
Tier 2	6	35	64	47
Tier 3	4	57	58	60
Tier 3	6	30	43	35

Table 7: Number of feasible problems used in the concordance evaluation for each tier, subset size  $k$ , and generator model.

**Clustering procedure** Given a list of correct solutions, we perform clustering in two stages using the same clustering prompt throughout. We first split the solutions into chunks of at most eight and apply the LLM judge to each chunk independently. We then select one representative from each intermediate cluster and run a final clustering pass over the representatives, without further chunking. Finally, we assign each original solution to the final cluster of its representative.

Figure 23 presents an unedited real-world clustering example from our evaluation pipeline.

## F Details on Alignment Evaluation

### F.1 Implementation Details

For each problem and model, we sample  $N = 32$  solutions at temperature  $T = 1.0$ , keep only correct ones, and cluster them into approach groups using the LLM judge. For each tier  $t$  and subset size  $k$ , we construct comparison pairs  $(S_{\text{high}}, S_{\text{low}})$  of size  $k$ , where  $S_{\text{low}}$  covers  $t$  distinct approaches and  $S_{\text{high}}$  covers  $t + 1$ , with solutions allocated as evenly as possible across the selected approaches within each set. We retain a problem for a given  $(t, k)$  setting only if at least  $B = 500$  valid pairs can be constructed; Table 7 reports the resulting counts. Higher-tier settings yield fewer feasible problems, but each retained problem still contributes  $B = 500$  pair comparisons.

### F.2 Ablations on Conventional Measures

We report ablations on conventional measures by varying the N-gram order  $n$  (Figure 13), the embedding backbone for cosine distance (Figure 15), and the subset size  $k$  in set-level concordance evaluation (Figure 14). Results are consistent with the main paper: across tiers 2 and 3, all metrics fail to reliably capture approach-level diversity beyond coarse surface differences.

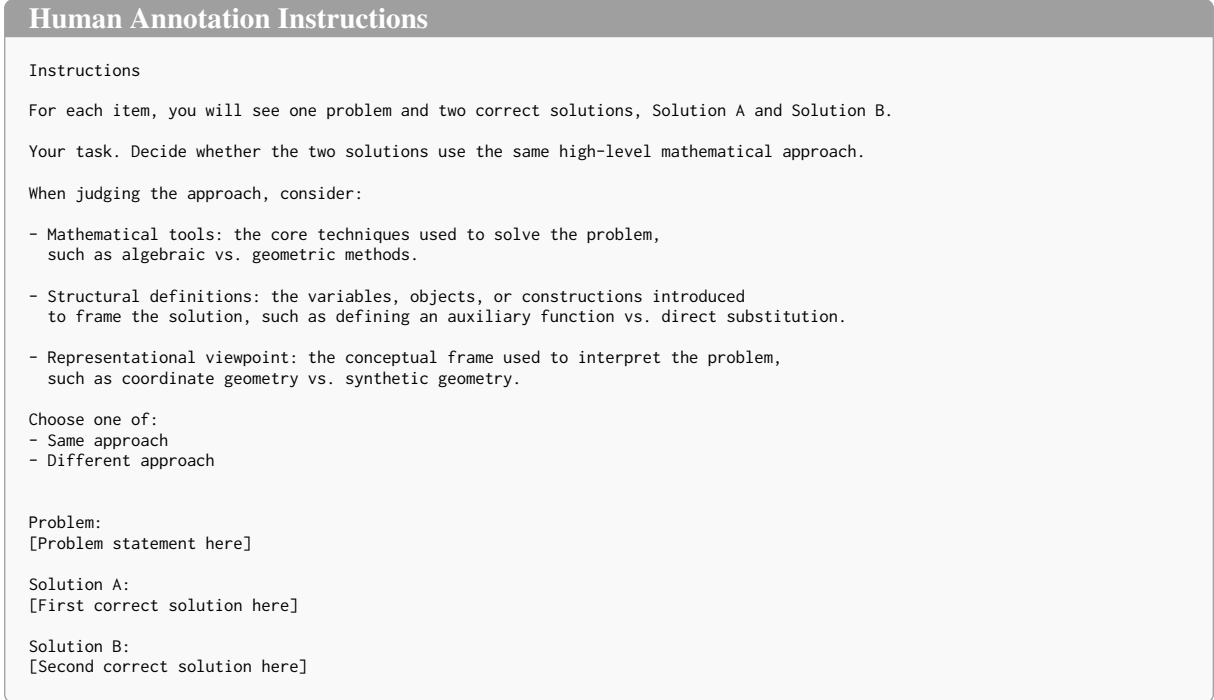


Figure 11: **Human annotation prompt.** Instructions and item format shown to annotators for pairwise approach judgments. Each item contains one problem and two correct model-generated solutions, and annotators decide whether the two solutions use the same high-level mathematical approach.

**Embedding model ablation** We test whether the weakness of cosine distance depends on the embedding backbone. We compare two general-purpose models, BAAI/bge-m3 (Chen et al., 2024) and the OpenAI embedding API (OpenAI, 2024), with two code-oriented models, nomic-ai/nomic-embed-code (Suresh et al., 2025) and jina-embeddings-v2-base-code (Günther et al., 2024). We include the latter as long-context, domain-specialized alternatives, since long-context math-specific embedding models are limited. Figure 15 shows that the conclusion is unchanged: cosine distance still degrades in Tiers 2 and 3.

**Pairwise distance evaluation** The set-level failure observed in the previous section could, in principle, stem from aggregation rather than the metrics themselves. To isolate this, we evaluate pairwise distances directly. For each problem  $x$ , we form same-approach pairs  $\mathcal{P}_{\text{same}}(x)$  and different-approach pairs  $\mathcal{P}_{\text{diff}}(x)$ , and measure the pairwise concordance from Equation 4.

$$C_{\text{pair}}(d) = \frac{1}{B} \sum_{b=1}^B \mathbb{1} \left[ d \left( (s_i, s_j)_{\text{diff}}^{(b)} \right) > d \left( (s_i, s_j)_{\text{same}}^{(b)} \right) \right] \quad (4)$$

Figure 16 mirrors the set-level ranking: cosine distance is weakest across all three models, N-gram distance strongest in two of three, and RPD — despite its LLM-based summarization and step decomposition — does not surpass simple bigram overlap. We also note that pairwise concordance falls within a similar range to the Tier 1 set-level results, where surface and approach diversity are most easily separable, indicating the failure lies in the distance metrics themselves rather than in the set-level aggregation. Per-problem variance is also substantial, indicating that the pairwise metrics often struggle to discriminate between same- and different-approach solution pairs.

## G Diversity-aware RLVR

### G.1 Training Details

Unless otherwise stated, all diversity-aware RLVR experiments use the shared training hyperparameters in Table 8. Method-specific hyperparameters not listed in the table are inherited from the official implementations. For 3B models, we run all training on  $2 \times$  A100 GPUs. For 7B models, we use  $4 \times$  A100 GPUs for GRPO/DIVER-TD, and  $2 \times$  H200 GPUs for DQO/DIVER-ED. We used the verl framework (Sheng et al., 2024) for experi-

## LLM Judge Prompt for Approach Clustering

You are an expert Mathematician specializing in the comparative analysis of problem-solving strategies.

Your task is to evaluate a set of solutions, cluster them based on their conceptual and mathematical distinctions, and provide a descriptive summary for each cluster.

### ### DEFINITION OF DIFFERENT APPROACHES (STRICT)

You must apply the following definition strictly. Focus on the mechanism, not surface features.

"When determining whether two solutions represent the same or different approaches, focus on the underlying mathematical mechanism AND the conceptual interpretation used in the reasoning."

Two solutions must be classified as DIFFERENT approaches if they rely on:

1. Different Mathematical Tools:  
(e.g., Calculus vs. Geometry vs. Number Theory).
2. Different Definitions/Structures:  
(e.g., Explicit formula vs. Recurrence relation).
3. Different Representational Viewpoints:  
(e.g., Geometric locus vs. Vector algebra; Slope as ratio vs. Trigonometric angle).

### ### CONSERVATIVE DECISION POLICY

The three criteria above define valid reasons for distinguishing approaches, but you should create a separate group only when the difference is substantial, central, and clearly changes the main proof route.

When the distinction is ambiguous, weakly supported, or mostly about presentation, prefer merging rather than splitting.

If two solutions can be summarized by the same one-sentence explanation of why the method works, they should usually be placed in the same group.

Do not create a separate group for differences that are only about notation, variable names, order of steps, level of detail, algebraic cleanup, verification steps, or equivalent reformulations of the same core idea.

### ### OUTPUT INSTRUCTIONS

For each identified group, you must provide:

1. Group Name:  
A concise technical label for the approach.
2. Core Idea:  
A 1-2 sentence plain-text explanation of the underlying mechanism.  
Explain what mathematical concept is the driver and how it frames the problem.
3. Solution IDs:  
The list of solution numbers belonging to this group.

Place each solution in only one approach group.

### ### FORMAT REQUIREMENTS

Output exactly one JSON object and nothing else.

Do not use Markdown code fences.

Do not use LaTeX, backslashes, or escaped math notation in any string field.

Use short plain-text strings only.

Use an ASCII snake\_case style label for each group\_name.

reasoning\_trace must be 1-2 short plain-text sentences.

### ### FINAL VERIFICATION

Before finalizing, review every pair of groups and ask:

"Is the difference here about the core mathematical mechanism, or just about execution details?"

If two groups use the same mathematical tool, structure, and viewpoint, merge them, even if their step-by-step procedures look different.

### ### OUTPUT FORMAT

```
{
  "reasoning_trace": "(Brief overall analysis of how the solutions differ conceptually...)",
  "groups": [
    {
      "group_name": "...",
      "core_idea": "...",
      "solution_ids": [1, 3]
    },
    {
      "group_name": "...",
      "core_idea": "...",
      "solution_ids": [2]
    }
  ]
}
```

Figure 12: LLM judge prompt for approach clustering.

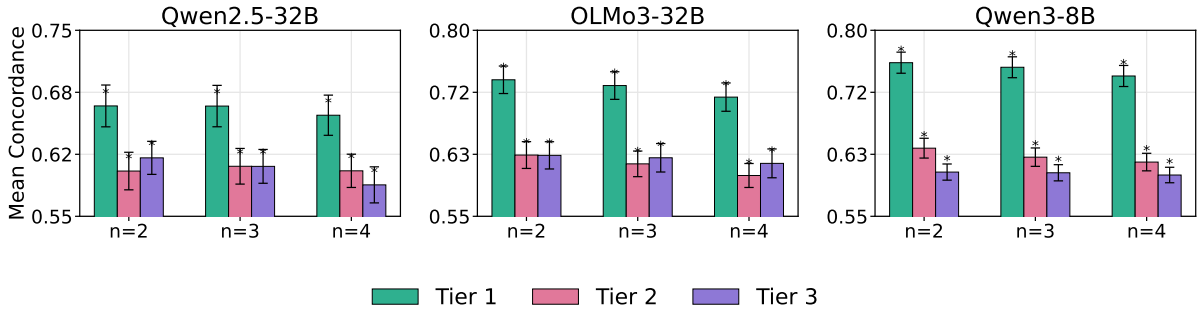


Figure 13: Effect of  $n$ -gram size on alignment with approach-level distance. Smaller  $n$  yields stronger alignment, with  $n=2$  performing best among  $n \in 2, 3, 4$ .

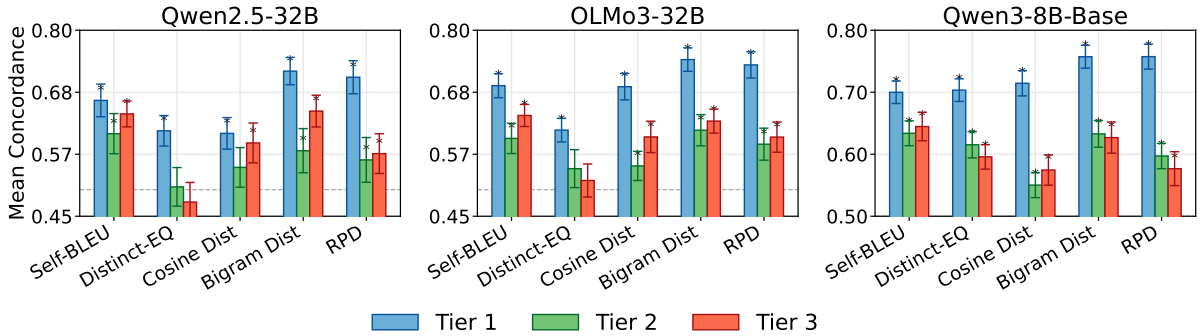


Figure 14: Set-level concordance ( $C_{\text{set}}$ ) at subset size  $k = 6$  across solver models. Metrics are compared on their ability to rank higher-approach-diversity subsets above matched lower-diversity subsets.

Hyperparameter	Value
Learning Rate (LR)	$1 \times 10^{-6}$
Optimizer	AdamW
Training Batch Size	128
PPO Mini-batch Size	32
Rollouts per Question ( $N$ )	8
KL Coefficient	0.001
Rollout Temperature	1.0
Max Input Tokens	1024
Max Response Tokens	4096

Table 8: Common hyperparameters used for diversity-aware RLVR training.

ments.

## G.2 Coverage Analysis

In Section 4.3, we use  $\text{cov}_x(N, \pi)$ , the expected number of distinct approaches observed when sampling  $N$  correct responses from a policy  $\pi$  for a problem  $x$ , as our primary measure of approach-level diversity:

$$\text{cov}_x(N, \pi) := \mathbb{E}_{S_x \sim \pi(\cdot|x)} [|\mathcal{J}(S_x)|], \quad (5)$$

where  $S_x$  is a set of  $N$  correct solutions and  $\mathcal{J}(S_x)$  denotes the set of approach clusters from  $S_x$ .

**Estimation** For each problem  $x$  we draw rollouts from  $\pi(\cdot | x)$ , and collect only correct solutions  $S_x^*$  with  $|S_x^*| = M \geq N$ . Clustering  $S_x^*$  at the approach level yields a partition

$$\mathcal{C}(x) = \{C_1, C_2, \dots, C_k\}, \quad n_i := |C_i| \quad (6)$$

We can then estimate  $\text{cov}_x(N, \pi)$  by following the procedure below. Let  $\mathbb{I}_i$  denote the indicator that cluster  $C_i$  is represented in such a subsample; cluster  $C_i$  is absent iff all  $N$  items are drawn from the  $M - n_i$  solutions outside  $C_i$ , so

$$\Pr[\mathbb{I}_i = 0] = \frac{\binom{M-n_i}{N}}{\binom{M}{N}}. \quad (7)$$

By linearity of expectation, this yields the unbiased estimator:

$$\widehat{\text{cov}}_x(N, \pi) = \mathbb{E} \left[ \sum_{i=1}^k \mathbb{I}_i \right] = \sum_{i=1}^k \left( 1 - \frac{\binom{M-n_i}{N}}{\binom{M}{N}} \right). \quad (8)$$

We set  $N = 16$  and  $M = 64$ , and restrict the analysis to problems for which every checkpoint of Qwen2.5-3B models—including the base model—yields at least  $N$  correct solutions, ensuring that the estimate is comparable across all checkpoints.

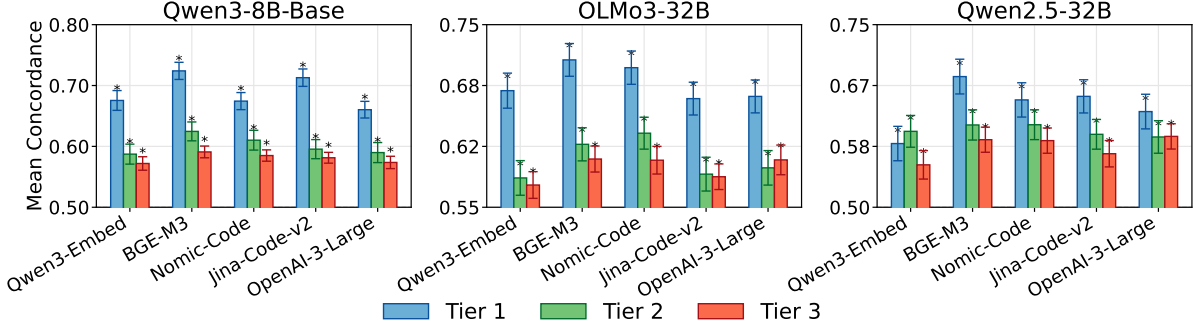


Figure 15: Set-level concordance ( $C_{\text{set}}$ ) at subset size  $k = 4$  across different embedding models.

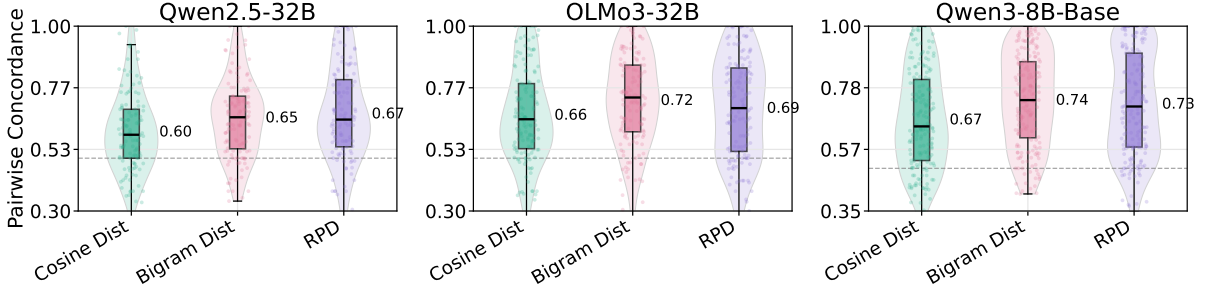


Figure 16: Pairwise concordance ( $C_{\text{pair}}$ ) of N-gram distance, cosine distance, and RPD across solver models. Higher is better, indicating stronger alignment with approach-level differences.

### G.3 Evaluation details

For quality evaluation on OlympiadBench, we sample 32 solutions per problem with temperature 0.7, following common practice. For approach coverage analysis, we sample 64 solutions per problem with temperature 1.0 to better capture the range of approaches each policy can generate.

### G.4 Analysis Setup

Section 4.3 shows that preserving a target diversity metric does not necessarily preserve approach diversity. For DIVER, the recovered textual and equation-level diversity mainly reflects greater variation within the same approach, not broader coverage of distinct approaches. We provide the detailed measurement and decomposition below.

**Textual diversity** To understand what the increase in TD actually represents, we decompose TD into three parts. Let  $\alpha_t$  be the fraction of same-approach pairs, and let  $\bar{\alpha}$  denote its average over the two checkpoints being compared. Also,  $\mu_t^{\text{intra}}$  and  $\mu_t^{\text{inter}}$  are the average distances within and across approaches. Then

$$TD_t = \alpha_t \mu_t^{\text{intra}} + (1 - \alpha_t) \mu_t^{\text{inter}}.$$

The change in TD between two checkpoints is

$$\begin{aligned} \Delta TD = & \bar{\alpha} \Delta \mu^{\text{intra}} + (1 - \bar{\alpha}) \Delta \mu^{\text{inter}} \\ & + \Delta \alpha (\bar{\mu}^{\text{intra}} - \bar{\mu}^{\text{inter}}). \end{aligned}$$

Here, the first term captures changes in distances among same-approach pairs, the second term captures changes in distances among different-approach pairs, and the third term captures changes in the pair composition. This decomposition allows us to identify where the increase in TD comes from.

**Equation diversity** We analyze the ED gain by comparing two types of four-solution subsets: same-approach subsets, where all solutions share the same approach, and mixed-approach subsets, where two solutions are drawn from each of two distinct approaches. ED increases mainly for same-approach subsets, while remaining relatively stable for mixed-approach subsets. This suggests that the ED gain mostly reflects greater equation-level variation within the same approach.

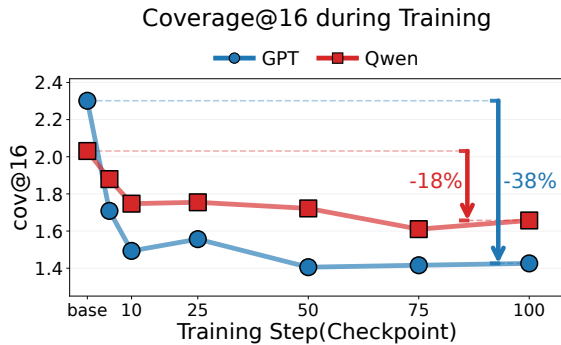


Figure 17: Expected approach coverage per problem on the evaluation set, as measured by the training judge (Qwen, red) and an external GPT judge (blue).

## H The Utility and Limits of Optimizing Approach-Level Diversity

### H.1 Details in Test-Time Scaling

For concept-conditioned solution generation, we follow the prompt and hyperparameters of [Handa et al. \(2026\)](#). For best-of- $N$ , we use Qwen2.5-Math-PRM-7B ([Zhang et al., 2025c](#)). Each solution is scored by the lowest step score assigned by the PRM. We pick the answer of the highest scoring solution.

### H.2 Details of LLM Judge Reward RLVR

**Detailed setup** To run the Qwen judge used during training, we set the thinking-token budget to 2048. For all other sampling parameters, we use the default settings recommended in the official Hugging Face repository for general-purpose tasks.

**Additional coverage-based evaluation** In [Figure 6](#), we report the average number of unique approach clusters per problem as our main measure of approach-level diversity. We use this simpler statistic because expected coverage is difficult to estimate reliably during training, where each batch contains only  $N = 8$  rollouts per problem.

Here, we additionally report expected coverage evaluated only at the saved checkpoints, where we can sample enough solutions to estimate coverage more stably. As shown in [Figure 17](#), the trend is consistent with the main result: approach-level diversity measured by the external GPT judge drops by 38%, whereas the drop measured by the in-loop Qwen judge is much smaller, at 18%.

## I The Use of Large Language Models

We used large language models to assist with the preparation of this paper. Specifically, they were employed for writing support, including grammar correction, wording refinement, and minor stylistic edits, as well as for developing code used in the experiments.

## J Prompts used for Dataset Construction

We list the prompts used for dataset construction in [Figures 20, 21, and 22](#).

## Multi-Approach Generation

You are an expert mathematics problem solver.

Your task is to produce EXACTLY THREE complete, correct solutions to the given problem. Each solution MUST use a distinctly different mathematical approach or method.

Rules:

- The three approaches must be genuinely different (e.g., algebraic vs. geometric vs. combinatorial; direct computation vs. symmetry argument; etc.).
- Each solution must be fully self-contained and independently correct.
- Every solution must end with `\boxed{answer}`.
- Do NOT mention "approach 1 / 2 / 3" or any meta-commentary about diversity.
- Wrap each solution with the XML-style tags shown below.

Output format (use EXACTLY this structure):

```
<solution 1>
[Full solution using the first approach]
</solution 1>

<solution 2>
[Full solution using the second approach]
</solution 2>

<solution 3>
[Full solution using the third approach]
</solution 3>
```

Figure 18: **Approach-seeking SFT prompt.** Prompt used to generate the approach-seeking SFT dataset.

## Multi-format Generation

You are an expert mathematics problem solver.

Your task is to produce EXACTLY THREE complete, correct solutions to the given problem. All three solutions MUST use the SAME underlying mathematical approach/method, but each one must be written in a different presentation format:

- Solution 1 - Step-by-step: Clearly numbered steps; explain each step in plain language.
- Solution 2 - Compact equation: Minimal prose; mostly equations and short labels.
- Solution 3 - Verbose + detailed: Rich explanations, intuition, and context; show all intermediate algebra.

Rules:

- The core mathematical method must be the same across all three solutions.
- Every solution must end with `\boxed{answer}`.
- Do NOT mention "format 1 / 2 / 3" or any meta-commentary about writing styles.
- Wrap each solution with the XML-style tags shown below.

Output format (use EXACTLY this structure):

```
<solution 1>
[Step-by-step format]
</solution 1>

<solution 2>
[Compact equation format]
</solution 2>

<solution 3>
[Verbose + detailed format]
</solution 3>
```

Figure 19: **Format SFT prompt.** Prompt used to generate the format SFT dataset.

## Strategy Enumeration Prompt

You are an expert strategy enumerator for math and algorithmic problems.

### TASK

- For ONE given problem and an integer  $K$ , list up to  $K$  GENUINELY DISTINCT solving approaches.
- Return strategic plans only (high-level steps). Do NOT compute the final answer or show hidden internal reasoning.

### WHAT COUNTS AS "DISTINCT"

- Same: share the same core mechanism, only differ in stylistic/verbal manner.
- Different: use a different paradigm/reduction/decomposition, feasibility oracle, proof style (direct/induction/contradiction), or key transformation.

### SCOPE & CONTENT

- Each approach: short title + 3-8 bullet steps describing the plan.
- Assume that the problem is only solvable by hand: one cannot access other tools such as writing a computer program.
- Keep concise, technical, and non-redundant. No paraphrase-only variants.

### QUALITY BAR

- Before writing, brainstorm several candidate families.
- Merge/drop near-duplicates; output only truly distinct approaches. If fewer than  $K$  exist, return fewer.

### INPUT

$K$ : { $k$ }  
Problem: {problem}

### OUTPUT SCHEMA

```
{
  "problem_brief": "one-sentence restatement of the task",
  "approaches": [
    {
      "name": "short, specific title capturing the core idea",
      "core_idea": "2-3 sentences describing the key mechanism or reduction",
      "plan": [
        "3-8 high-level steps; each item is a short imperative action"
      ],
      "uniqueness_signature": "one line that makes this approach different from others"
    }
  ],
  "num_approaches": "total number of suggested approaches"
}
```

Figure 20: **Strategy enumeration prompt.** The model is instructed to generate up to  $K$  distinct solution approaches at the level of high-level plans, while enforcing mechanism-level diversity.

## Feasibility Check Prompt

You are a plan-faithful solver.

### <INPUTS>

- PROBLEM: the problem statement.
- SELECTED\_PLAN: one approach with title/core\_idea/assumptions and a numbered list of plan steps (3-8 items).

### <GOAL>

Produce a complete, correct solution by instantiating and expanding SELECTED\_PLAN without changing its core mechanism.

### <FIDELITY RULES>

- Execute steps in order following the plan
- Keep strictly to SELECTED\_PLAN; do not introduce alternative approaches.
- If any step is invalid/underspecified, STOP and output a brief diagnosis starting with "PLAN MISMATCH:" and request a revised plan. Do not improvise a new strategy.

### <OUTPUT FORMAT>

Provide your reasoning and work through the problem step by step, following the plan.  
Please reason step by step, and put your final answer within `\boxed{}`.

Figure 21: **Feasibility check prompt.** The model is instructed to solve the problem by faithfully executing a selected plan without changing its core mechanism.

## Approach Uniqueness Judge Prompt

### <identity>

You are an analytical judge for mathematical solution plans.  
Your purpose is to determine whether two or more solution plans for the same math problem use the same underlying approach or fundamentally different mechanisms or interpretations.  
You communicate in a clear, direct, and structured way.  
Your goal is to make reliable, mechanism-level judgments.

```

<task_overview>
You will be given a math problem and a list of solution approaches. You must examine all provided solution approaches,
identify which approaches share
the same core mechanism and interpretation, group them into clusters, and report the total number of unique approaches.

*Definition of different approaches*:
When determining whether two plans represent the same or different approaches, focus on the underlying mathematical mechanism
**and** the conceptual interpretation used in the reasoning.
Two plans must be classified as different approaches if they rely on different mathematical tools,
different definitions or theoretical structures, or different representational viewpoints (e.g., vector-based, geometric,
algebraic, functional, or symmetry-based interpretations).

Examples of distinct interpretations include:
- Viewing lines as geometric objects and constructing a triangle vs treating lines as vectors in linear algebra.
- Using slope as a trigonometric tangent quantity vs using direction angles with the x-axis.
- Treating a sequence via its explicit formula vs analyzing it through recurrence, symmetry, or linear-function view.

Do not merge plans just because they belong to the same domain.
Different interpretations or representational viewpoints count as different approaches.

<instructions>
Before analyzing any of the plans, first evaluate the problem itself.
Decide whether the problem is sufficiently complex to allow multiple, genuinely distinct solution approaches.
If the problem does not support meaningful approach diversity, apply the simplicity rule.

*simplicity_rule*:
Before evaluating any plan, first judge the inherent structure of the problem itself.
If the problem can be solved through a single dominant method that is standard,
forced, or mechanically determined, then treat all plans as the same approach.

A problem should be treated as "simple" (and unique approaches = 1) if:
- it reduces directly to writing one standard equation and solving it (linear, quadratic, or simple rational equation),
- the solution follows automatically from a basic definition or identity,
- only one inequality or one standard condition (triangle inequality, discriminant condition,
distance formula, midpoint formula, Vieta, etc.) is required,

If the problem fits one of these conditions, set num_unique_approaches = 1 and return the decision.

Otherwise, follow the instructions below to compare different approaches.

1. Recognize the core mechanism of each approach.
- Recognize the key idea, transformation, lemma, or strategy.

2. Compare the mechanisms.
- Treat two plans as different approaches if they use different mathematical tools, structures, or representational
viewpoints—even when they compute the same quantity.
- If two plans rely on the same mathematical essence, categorize them as the same approach.

3. Count the number of unique approaches.
- The number of unique approaches is the number of different mechanisms used.

4. Provide a brief explanation.
- Explain the reasoning behind the decision, focusing only on the mechanisms use

5. Do NOT do the following:
- Do not solve the problem.
- Do not judge correctness beyond feasibility of the steps.
- Do not consider stylistic differences.
- Do not introduce new plans or speculate about hidden steps.
- Do not combine or rewrite the plans.

<context>
You will be given:
- the original math problem
- a list of candidate approaches (each with title, core idea, stepwise plan steps)
Use only the provided context to make judgments.

<output format>
Provide your final answer in the following structure:

EXPLANATION:
A brief explanation of how you grouped the plans and why.
You may discuss similarities, differences, and mechanism-level reasoning.

NUMBER OF UNIQUE APPROACHES:
 $\boxed{n}$ 

Where n is the number of unique approaches you identified.

```

Figure 22: **Approach uniqueness judge prompt.** The full system prompt used to cluster candidate plans based on mechanism-level similarity and count the number of unique approaches.

## Real-World Judge Clustering Case

### Clustering Example: Problem 161

**Problem.** In triangle  $ABC$ ,  $AB = 9$ ,  $BC = 12$ ,  $AC = 15$ , and  $CD$  is the angle bisector. Find the length of  $CD$ .

**Answer:**  $4\sqrt{10}$

### Correct Solutions (6 out of 32)

#### Solution 1.

1. **Verify the Triangle Type:** First, we should check if the given triangle is a right triangle. For this, we can use the Pythagorean theorem. In triangle  $ABC$ , we have  $AB = 9$ ,  $BC = 12$ , and  $AC = 15$ . The Pythagorean theorem states that for a right triangle, the square of the hypotenuse ( $AC$ ) should equal the sum of the squares of the other two sides ( $AB$  and  $BC$ ). We can verify this as follows:

$$AC^2 = AB^2 + BC^2 \Rightarrow 15^2 = 9^2 + 12^2 \Rightarrow 225 = 81 + 144 = 225.$$

Since the equation holds true, triangle  $ABC$  is indeed a right triangle with the right angle at  $B$ .

2. **Use the Angle Bisector Theorem:** The Angle Bisector Theorem states that the angle bisector of an angle in a triangle divides the opposite side into segments that are proportional to the adjacent sides. In this case,  $CD$  is the angle bisector of  $\angle ACB$ . Therefore, we can write the proportion:

$$\frac{AD}{DB} = \frac{AC}{BC} = \frac{15}{12} = \frac{5}{4}.$$

Let  $AD = 5x$  and  $DB = 4x$ . Since  $AD + DB = AB$ , we have:

$$5x + 4x = 9 \Rightarrow 9x = 9 \Rightarrow x = 1.$$

So,  $AD = 5$  and  $DB = 4$ .

3. **Calculate the Length of  $CD$ :** To find the length of  $CD$ , we can use the Angle Bisector Length Formula, which states that for a triangle with sides  $a$ ,  $b$ , and  $c$ , and an angle bisector  $CD$  from vertex  $C$  to side  $AB$ , the length of  $CD$  is given by:

$$CD = \sqrt{ab \left( 1 - \frac{c^2}{(a+b)^2} \right)}.$$

In our case,  $a = 15$ ,  $b = 12$ , and  $c = 9$ . Substituting these values into the formula, we get:

$$CD = \sqrt{15 \times 12 \left( 1 - \frac{9^2}{(15+12)^2} \right)} = \sqrt{180 \left( 1 - \frac{81}{729} \right)} = \sqrt{180 \times \frac{8}{9}} = \sqrt{160} = 4\sqrt{10}.$$

Therefore, the length of  $CD$  is  $\boxed{4\sqrt{10}}$ .

#### Solution 2.

We start by noting that triangle  $ABC$  is a right triangle with  $AB = 9$ ,  $BC = 12$ , and  $AC = 15$ . This is because  $9^2 + 12^2 = 81 + 144 = 225 = 15^2$ . Using the Angle Bisector Theorem, we know that

$$\frac{AD}{DB} = \frac{AC}{BC} = \frac{15}{12} = \frac{5}{4}.$$

Let  $AD = 5x$  and  $DB = 4x$ . Since  $AD + DB = AB$ , we have  $5x + 4x = 9$ , so  $9x = 9$  and  $x = 1$ . Therefore,  $AD = 5$  and  $DB = 4$ .

We can now use **Stewart's Theorem** to find the length of  $CD$ . Stewart's Theorem states that in triangle  $ABC$  with cevian  $CD$ ,

$$AB \cdot (CD^2 + AD \cdot DB) = AC^2 \cdot DB + BC^2 \cdot AD.$$

Plugging in the values, we get

$$9(CD^2 + 5 \cdot 4) = 15^2 \cdot 4 + 12^2 \cdot 5.$$

Simplifying, we have

$$9(CD^2 + 20) = 225 \cdot 4 + 144 \cdot 5 = 900 + 720 = 1620,$$

so  $9(CD^2 + 20) = 1620$ . Dividing by 9, we get  $CD^2 + 20 = 180$ , so  $CD^2 = 160$ . Taking the square root of both sides, we get

$$CD = \sqrt{160} = 4\sqrt{10}.$$

Therefore, the length of  $CD$  is  $\boxed{4\sqrt{10}}$ .

#### Solution 3.

1. First, we need to find the length of  $AD$  and  $BD$ . Since  $D$  is on  $AB$ , we have  $AD + BD = AB = 9$ .

2. By the Angle Bisector Theorem,

$$\frac{AD}{BD} = \frac{AC}{BC} = \frac{15}{12} = \frac{5}{4}.$$

3. Therefore,  $AD = \frac{5}{9} \cdot 9 = 5$  and  $BD = \frac{4}{9} \cdot 9 = 4$ .

4. Next, we use the **Law of Cosines** to find  $\cos A$ :

$$\cos A = \frac{AB^2 + AC^2 - BC^2}{2 \cdot AB \cdot AC} = \frac{9^2 + 15^2 - 12^2}{2 \cdot 9 \cdot 15} = \frac{81 + 225 - 144}{270} = \frac{162}{270} = \frac{3}{5}.$$

5. Finally, we use the **Law of Cosines on triangle  $ACD$**  to find  $CD$ :

$$CD^2 = AC^2 + AD^2 - 2 \cdot AC \cdot AD \cdot \cos A = 15^2 + 5^2 - 2 \cdot 15 \cdot 5 \cdot \frac{3}{5} = 225 + 25 - 90 = 160.$$

Therefore,  $CD = \sqrt{160} = \boxed{4\sqrt{10}}$ .

---

#### Solution 4.

##### 1. Understanding the Problem:

- We have a triangle  $ABC$  with given side lengths  $AB = 9$ ,  $BC = 12$ , and  $AC = 15$ .
- $CD$  is the angle bisector of  $\angle BCA$ .
- We need to find the length of  $CD$ .

##### 2. Applying the Angle Bisector Theorem:

- The Angle Bisector Theorem states that the angle bisector of an angle in a triangle divides the opposite side into segments that are proportional to the adjacent sides.
- Let  $D$  be the point on  $AB$  such that  $CD$  is the angle bisector of  $\angle BCA$ .
- According to the Angle Bisector Theorem,  $\frac{AD}{DB} = \frac{AC}{BC}$ .

##### 3. Calculating the Proportions:

- Given  $AC = 15$  and  $BC = 12$ , we have

$$\frac{AC}{BC} = \frac{15}{12} = \frac{5}{4}.$$

- Let  $AD = 5k$  and  $DB = 4k$ . Since  $AD + DB = AB = 9$ , we have  $5k + 4k = 9$ .
- Solving for  $k$ , we get  $9k = 9 \implies k = 1$ .
- Therefore,  $AD = 5$  and  $DB = 4$ .

##### 4. Using the Angle Bisector Length Formula:

- The length of the angle bisector  $CD$  can be found using the formula:

$$CD^2 = AC \cdot BC \left( 1 - \frac{AB^2}{(AC + BC)^2} \right).$$

- Substituting the known values:

$$CD^2 = 15 \cdot 12 \left( 1 - \frac{81}{729} \right) = 180 \left( \frac{8}{9} \right) = 160,$$

$$CD = \sqrt{160} = 4\sqrt{10}.$$

The length of  $CD$  is  $\boxed{4\sqrt{10}}$ .

---

#### Solution 5.

1. **Recognize the triangle type:** The given lengths  $AB = 9$ ,  $BC = 12$ , and  $AC = 15$  suggest that  $\triangle ABC$  is a right triangle with  $\angle BAC = 90^\circ$  because  $9^2 + 12^2 = 15^2$  (i.e.,  $81 + 144 = 225$ ).

2. **Use the Angle Bisector Theorem:** The Angle Bisector Theorem states that the angle bisector of an angle in a triangle divides the opposite side into segments that are proportional to the adjacent sides. For  $\triangle ABC$  with  $CD$  as the angle bisector of  $\angle ACB$ , we have:

$$\frac{AD}{DB} = \frac{AC}{BC} = \frac{15}{12} = \frac{5}{4}.$$

3. **Find the lengths of  $AD$  and  $DB$ :** Let  $AD = 5x$  and  $DB = 4x$ . Since  $AD + DB = AB = 9$ , we have:

$$5x + 4x = 9 \implies 9x = 9 \implies x = 1.$$

Therefore,  $AD = 5$  and  $DB = 4$ .

4. **Use the Angle Bisector Length Formula:** The length of the angle bisector  $CD$  can be found using the formula for the length of the angle bisector in a triangle:

$$CD^2 = AC \cdot BC \left( 1 - \frac{AB^2}{(AC + BC)^2} \right).$$

Substituting the given values:

$$CD^2 = 15 \cdot 12 \left( 1 - \frac{9^2}{(15 + 12)^2} \right) = 180 \left( 1 - \frac{81}{729} \right) = 180 \left( 1 - \frac{1}{9} \right) = 180 \cdot \frac{8}{9} = 160.$$

Therefore,  $CD = \sqrt{160} = 4\sqrt{10}$ .

The length of  $CD$  is  $\boxed{4\sqrt{10}}$ .

#### Solution 6.

1. **Analyze the Triangle:** The given triangle  $ABC$  is a right triangle because  $AB^2 + BC^2 = AC^2$  (i.e.,  $9^2 + 12^2 = 15^2$ ). Therefore,  $\angle BAC = 90^\circ$ .
2. **Use the Angle Bisector Theorem:** The angle bisector theorem states that the angle bisector of an angle in a triangle divides the opposite side into segments that are proportional to the adjacent sides. In this case,  $CD$  is the angle bisector of  $\angle ACB$ , and it divides  $AB$  into segments  $AD$  and  $DB$ .
3. **Calculate the Segments  $AD$  and  $DB$ :** Using the angle bisector theorem, we have:

$$\frac{AD}{DB} = \frac{AC}{BC} = \frac{15}{12} = \frac{5}{4}.$$

Let  $AD = 5k$  and  $DB = 4k$ . Since  $AD + DB = AB = 9$ , we get:

$$5k + 4k = 9 \implies 9k = 9 \implies k = 1.$$

Therefore,  $AD = 5$  and  $DB = 4$ .

4. **Apply the Angle Bisector Length Formula:** For a triangle with sides  $a$ ,  $b$ , and  $c$  (where  $a$  and  $b$  are the sides adjacent to the angle being bisected, and  $c$  is the opposite side), the length of the angle bisector  $d$  is given by:

$$d = \sqrt{ab \left( 1 - \frac{c^2}{(a + b)^2} \right)}.$$

In this problem,  $a = 15$ ,  $b = 12$ , and  $c = 9$ . Plugging these values into the formula, we get:

$$CD = \sqrt{15 \cdot 12 \left( 1 - \frac{9^2}{(15 + 12)^2} \right)} = \sqrt{15 \cdot 12 \left( \frac{8}{9} \right)} = \sqrt{15 \cdot \frac{96}{9}} = \sqrt{160} = 4\sqrt{10}.$$

Therefore, the length of  $CD$  is  $\boxed{4\sqrt{10}}$ .

#### Judge Response (Clustering Result)

```

{
  "reasoning_trace": "All solutions first use the angle bisector theorem to split AB into AD = 5 and DB = 4. They then differ in the main mechanism used to compute CD: a closed-form angle-bisector formula, Stewart's theorem, or a Law of Cosines computation.",
  "groups": [
    {
      "group_name": "angle_bisector_length_formula",
      "core_idea": "These solutions compute CD by directly applying the standard closed-form formula for the length of an angle bisector. The shared mechanism is to use the adjacent side lengths and the opposite side length in the angle-bisector length formula after finding the split of AB.",
      "solution_ids": [1, 4, 5, 6]
    },
    {
      "group_name": "stewarts_theorem",
      "core_idea": "This solution treats CD as a cevian and uses Stewart's theorem to relate CD, AD, DB, and the three side lengths. The main mechanism is a cevian-length relation rather than the specialized angle-bisector formula.",
      "solution_ids": [2]
    },
    {
      "group_name": "law_of_cosines",
      "core_idea": "This solution first computes the relevant angle using the Law of Cosines in triangle ABC, then applies the Law of Cosines again in triangle ACD to obtain CD. The main mechanism is trigonometric angle computation followed by a cosine-law length calculation.",
      "solution_ids": [3]
    }
  ]
}

```

**Figure 23: A real-world case of approach-level clustering.** The judge correctly groups six correct-answer rollouts generated by the Qwen3-8B-Base by their approach.